

# 学位論文

**HE4 Predicts Progressive Fibrosis and Cardiovascular Events in Patients  
with Dilated Cardiomyopathy**  
(Human Epididymis Protein 4は拡張型心筋症における進行性の間質線維化に寄与し  
心血管予後を予測する)

山本 正啓

Masahiro Yamamoto

指導教員

辻田 賢一 教授

熊本大学大学院医学教育部博士課程医学専攻循環器内科学

2021 年度

# 学 位 論 文

論文題名 : **HE4 Predicts Progressive Fibrosis and Cardiovascular Events in Patients  
with Dilated Cardiomyopathy**

(Human Epididymis Protein 4は拡張型心筋症における進行性の間質線維化に寄与し心血管予後を予測する)

著者名 : 山本正啓  
Masahiro Yamamoto

指導教員名 : 熊本大学大学院医学教育部博士課程医学専攻循環器内科学 辻田賢一 教授

審査委員名 : 腎臓内科学担当教授 向山政志

細胞病理学担当教授 菰原義弘





生体機能薬理学担当教授 光山勝慶

代謝内科学担当教授 荒木栄一

2021年度

ORIGINAL RESEARCH

# HE4 Predicts Progressive Fibrosis and Cardiovascular Events in Patients With Dilated Cardiomyopathy

Masahiro Yamamoto, MD; Shinsuke Hanatani , MD, PhD; Satoshi Araki, MD, PhD; Yasuhiro Izumiya, MD, PhD; Toshihiro Yamada, MD; Nobuhiro Nakanishi, MD; Toshifumi Ishida, MD; Satoru Yamamura, MD, PhD; Yuichi Kimura, MD, PhD; Yuichiro Arima, MD, PhD; Taishi Nakamura , MD, PhD; Seiji Takashio, MD, PhD; Eiichiro Yamamoto, MD, PhD; Kenji Sakamoto, MD, PhD; Koichi Kaikita , MD, PhD; Kenichi Matsushita, MD, PhD; Sachio Morimoto , PhD; Takaaki Ito, MD, PhD; Kenichi Tsujita, MD, PhD

**BACKGROUND:** Cardiac fibrosis plays a crucial role in the pathogenesis of dilated cardiomyopathy (DCM). HE4 (human epididymis protein 4) is a secretory protein expressed in activated fibroblasts that exacerbates tissue fibrosis. In the present study, we investigated the clinical utility of HE4 measurement in patients with DCM and its pathophysiological role in preclinical experiments in vivo and in vitro.

**METHODS AND RESULTS:** We measured serum HE4 levels of 87 patients with DCM. Endomyocardial biopsy expressed severe fibrosis only in the high HE4 group ( $P < 0.0001$ ). Echocardiography showed that left ventricular end-diastolic diameter tends to decrease over time ( $58 \pm 7.3$  to  $51 \pm 6.6$  mm;  $P < 0.0001$ ) in the low HE4 group ( $< 59.65$  pmol/L [median value]). HE4 was significantly associated with risk reduction of mortality and cardiovascular hospitalization in multivariate Cox model. In vivo, HE4 was highly expressed in kidney and lung tissue of mouse, and scarcely expressed in heart. In genetically induced DCM mouse model, HE4 expression increased in kidney but not in heart and lung. In vitro, supernatant from HE4-transfected human embryonic kidney 293T cells enhanced transdifferentiation of rat neonatal fibroblasts and increased expression of fibrosis-related genes, and this was accompanied by the activation of extracellular signal-regulated kinase signaling in cardiac fibroblasts. Treatment with an inhibitor of upstream signal of extracellular signal-regulated kinase or a neutralizing HE4 antibody canceled the profibrotic properties of HE4.

**CONCLUSIONS:** HE4 functions as a secretory factor, activating cardiac fibroblasts, thereby inducing cardiac interstitial fibrosis. HE4 could be a promising biomarker for assessing ongoing fibrosis and a novel therapeutic target in DCM.

**REGISTRATION:** URL: <https://upload.umin.ac.jp/cgi-open-bin/ctr/>; Unique identifier: UMIN000043062.

**Key Words:** cardiorenal syndrome ■ HE4 (human epididymis protein 4) ■ left ventricular reverse remodeling ■ myofibroblast

**D**ilated cardiomyopathy (DCM) is one of the most common causes of heart failure (HF) and is associated with significant morbidity and mortality.<sup>1</sup> Pathophysiological remodeling of the left ventricle is an important hallmark of DCM, and one of the most important indicators of adverse events.<sup>2</sup> Furthermore,

left ventricular reverse remodeling (LVRR), characterized by a decrease in dimensions and normalization of shape, is associated with significant improvement in pump function and a favorable prognosis.<sup>3</sup> However, the causes and predictive variables of left ventricular (LV) remodeling and LVRR remain undetermined.<sup>4</sup>

Correspondence to: Shinsuke Hanatani, MD, PhD, Department of Cardiovascular Medicine, Graduate School of Medical Sciences, Kumamoto University, Honjo, Kumamoto 860-8556, Japan. E-mail: s-hanata@kumamoto-u.ac.jp

Supplementary Material for this article is available at <https://www.ahajournals.org/doi/suppl/10.1161/JAHA.120.021069>

For Sources of Funding and Disclosures, see page 12.

© 2021 The Authors. Published on behalf of the American Heart Association, Inc., by Wiley. This is an open access article under the terms of the Creative Commons Attribution-NonCommercial-NoDerivs License, which permits use and distribution in any medium, provided the original work is properly cited, the use is non-commercial and no modifications or adaptations are made.

JAHA is available at: [www.ahajournals.org/journal/jaha](http://www.ahajournals.org/journal/jaha)

## CLINICAL PERSPECTIVE

### What Is New?

- Low levels of serum HE4 (human epididymis protein 4) were significantly associated with future left ventricular reverse remodeling and favorable outcomes in patients with dilated cardiomyopathy.
- HE4 is upregulated at kidney tissue in heart failure with reduced ejection fraction model mice.
- The supernatant from HE4-transfected human embryonic kidney 293T cells introduced cardiac fibroblast activation and upregulation of fibrosis-related genes, which were accompanied by the activation of extracellular signal-regulated kinase signaling.

### What Are the Clinical Implications?

- HE4 is a key regulator of novel cardiorenal interaction and ongoing fibrosis of cardiac tissue, and can be a new biomarker contributing to a novel treatment strategy aimed at left ventricular reverse remodeling in patients with dilated cardiomyopathy.
- The data of present study suggest that HE4 could be a novel therapeutic target in dilated cardiomyopathy.

## Nonstandard Abbreviations and Acronyms

<b>DCM</b>	dilated cardiomyopathy
<b>ERK</b>	extracellular signal-regulated kinase
<b>HE4</b>	human epididymis protein 4
<b>HEK293T</b>	human embryonic kidney 293T
<b>HFrEF</b>	heart failure with reduced ejection fraction
<b>LVEDD</b>	left ventricular end-diastolic diameter
<b>LVEDVi</b>	left ventricular end-diastolic volume index
<b>LVESVi</b>	left ventricular end-systolic volume index
<b>LVRR</b>	left ventricular reverse remodeling
<b>WT</b>	wild type
<b>αSMA</b>	α-smooth muscle actin

A key cellular event in the pathophysiology of cardiac fibrosis and remodeling is activation of fibroblasts with subsequent deposition of extracellular matrix proteins.<sup>5</sup> Fibroblasts are activated in response to various stress stimuli, which facilitates their differentiation into myofibroblasts that express α-smooth muscle actin (αSMA).<sup>6</sup> Myofibroblasts excessively secrete

extracellular matrix proteins, leading to development of DCM.<sup>7</sup> Therefore, a noninvasive test to determine the expression of myofibroblasts has the potential to evaluate the degree or severity of “ongoing” fibrosis in patients with DCM. Late gadolinium enhancement via cardiac magnetic resonance (CMR) imaging is an effective tool for detection of myocardial fibrosis and one of the most useful modalities contributing to the diagnosis of DCM.<sup>2</sup> However, late gadolinium enhancement is not ideal in the evaluation of ongoing tissue fibrosis, as it has been shown to reflect “accomplished” myocardial fibrosis.<sup>8</sup>

Recent studies showed that HE4 (human epididymis protein 4), also known as WAP (whey acidic protein) 4-disulfide core domain 2, is specifically expressed by activated myofibroblasts and secreted into the circulation.<sup>9</sup> Its concentration in the serum of patients with renal diseases correlates with renal fibrosis, and treatment of mice with anti-HE4 antibodies was shown to improve renal fibrosis by reducing the multiple protease inhibitor activity characteristic of HE4.<sup>9</sup> In the current study, we measured circulating serum HE4 concentration in patients with DCM to determine its utility in the detection of ongoing cardiac fibrosis and future LV remodeling or adverse cardiac events. In addition, to determine whether HE4 has an impact on cardiac fibrosis, we conducted both in vivo and in vitro experiments.

## METHODS

For each paragraph, additional details can be found in Data S1. The data that support the findings of this study are available from the corresponding author on reasonable request.

### Study Population of Clinical Study

Eighty-seven consecutive patients with DCM, scheduled to undergo cardiac catheterization for an assessment of hemodynamic status or a diagnostic workup for HF at Kumamoto University Hospital between January 2009 and December 2018, were enrolled (Figure S1). DCM was diagnosed on the basis of clinical and physical examination, including enhanced CMR and myocardial biopsy. Of 87 patients, 60 (69%) underwent myocardial biopsy, and 2 cases showed lymphocyte infiltration suggestive of inflammatory dilated cardiomyopathy. HF was defined by the American College of Cardiology/American Heart Association, and only those with HF stage B or C were included.<sup>10</sup> Patients with neoplasms and those on hemodialysis were excluded. Fifty-nine patients without HF, confirmed by normal coronary angiography on cardiac catheterization, comprised our control group.

## Ethical Statement

All procedures were conducted in accordance with the Declaration of Helsinki and its amendments. The study protocol was approved by the institutional review board of Kumamoto University (approval No.: Senshin 2259). Opt-out materials are available at: <https://kumadai-junnai.com/archives/clinical>.

## Procedures

Blood samples were collected in the stable phase during the first admission, and the serum HE4 levels were measured using the Clinical Laboratory Improvement Amendments method (Abbott).

## Follow-Up and Study End Points

After baseline blood sampling, patients were followed up in the outpatient clinic for a median of 897 days (interquartile range, 421–3022 days). The study primary end point was a composite of all-cause death, LV assist device implantation, and hospitalization for HF events. Furthermore, a composite of all-cause death and LV assist device implantation was defined as secondary end point.

## Echocardiography

Echocardiography was performed under stable conditions on admission and during the follow-up period (median follow-up period, 639 days) (Vivid 7; GE-Vingmed Ultrasound). Changes over time in LV dimension and systolic function were evaluated by serial echocardiography measurements. Echocardiographic parameters were assessed in alignment with the recommendations of the American Society of Echocardiography.<sup>11</sup> LV end-diastolic diameter (LVEDD) index was calculated as LVEDD divided by body surface area. LV end-diastolic volume index (LVEDVi) and LV end-systolic volume index (LVESVi) were calculated as LV end-diastolic volume and LV end-systolic volume divided by body surface area. LV ejection fraction (LVEF) was calculated by the modified Simpson method (Vivid 7; GE-Vingmed Ultrasound).

## Statistical Analysis of Echocardiographic Data

Sixty-five patients (74%) underwent follow-up echocardiography and were analyzed by the degree of changes in echocardiographic parameters. Univariable linear regression, logistic regression, and multivariable analysis for  $\Delta$ LVEDVi (follow-up LVEDVi–baseline LVEDVi),  $\Delta$ LVESVi (follow-up LVESVi–baseline LVESVi), and LVRR was performed using HE4 and other variables involved in LV remodeling.<sup>12</sup> LVRR was defined as the combined presence of the following: (1) an increase

in LVEF of at least 10 points or a follow-up LVEF  $\geq$ 50%; and (2) a decrease in LVEDD index of at least 10% or an LVEDD index  $\leq$ 33 mm/m.<sup>3</sup>

## CMR Image Acquisition and Image Analysis

Sixty-six patients (76%) underwent CMR and were checked for the presence of late gadolinium enhancement.

## Myocardial Biopsy and Calculation of Collagen Volume Fraction and Extracellular Space

The samples were taken from the mid interventricular septum, and at least 2 samples per patient were submitted for light microscopic examination. All biopsy specimens were stained with Masson trichrome. The collagen area and total myocardial area were measured, and the collagen area fraction was expressed as percentage of total area. (ImageJ version 1.52a).

## Mouse Models and Procedures

Wild-type (WT) male mice and genetically induced DCM model mice on a BALB/cA background were used in this study. All procedures were performed in accordance with the Kumamoto University animal care guidelines, which conform to the *Guide for the Care and Use of Laboratory Animals*, published by the US National Institutes of Health (publication No. 85-23, revised 1996). The study was approved by the Animal Research Ethics Committee of Kumamoto University (No. A2019-122). WT male mice with BALB/cA background were purchased from Kyudo Company. The mice were anesthetized with isoflurane in all models. Two models of mouse HF with reduced ejection fraction (HFREF) were produced. The mouse myocardial infarction model was generated as previously described.<sup>13,14</sup> The mouse DCM model was generated using knock-in mice on the genetic background of BALB/cJ, in which 3 base pairs coding for K210 in cardiac troponin T were deleted from the endogenous *Tnnt2* gene, as previously described.<sup>15</sup> At 6-week-old WT mouse, at 4 weeks after myocardial infarction surgery mouse, and at 6-week-old DCM model mouse were anesthetized with overdose isoflurane, and hearts, kidney, lung, and liver were rapidly excised, and freeze clamped for subsequent analyses.

## Echocardiography, In Vivo

At 1 day before harvest, echocardiography was performed using the Xario system (Toshiba) with a 12-MHz linear array transducer.

## Cell Culture and Harvest and Incubation of Neonatal Rat Cardiomyocytes and Fibroblasts

Primary neonatal rat cardiomyocytes and fibroblasts were isolated from 2-day-old Wistar rats (Japan SLC, Inc), as described previously.<sup>14</sup> Cardiomyocyte and fibroblast isolation and primary culture were approved by the Committee on the Use of Live Animals in Research in Kumamoto University.

## Cell Culture, Transfection of Plasmid in Human Embryonic Kidney 293T Cells, and Culture Supernatant Transfer

Human embryonic kidney 293T (HEK293T) cells were cultured in high-glucose (4-g/L) DMEM containing 10% fetal bovine serum. The dish was replaced with fresh low-glucose DMEM with 0.1% fetal bovine serum, and then the control or HE4 plasmid (pcDNA3-HE4, No. 18101, Addgene) was introduced into HEK293T cells using Lipofectamine 3000 (Life Technologies), according to the manufacturer's instructions. The pcDNA3-HE4 was a gift from Ronny Drapkin (Addgene plasmid No. 18101; <http://n2t.net/addgene:18101>; Research Resource Identifier: Addgene\_18101). At 12 hours after transfection, the medium was replaced with fresh DMEM with 0.1% fetal bovine serum. After 24 hours, the culture supernatant from the HEK293T cells was transferred to previously harvested rat neonatal cardiomyocytes and cardiac fibroblasts. In addition, U0126 (No. 9903S, CST), an mitogen-activated protein kinase (MEK)1/2 inhibitor, was used to inhibit the phosphorylation of extracellular signal-regulated kinase (ERK) in rat neonatal cardiac fibroblasts. Anti-HE4 antibody (ab200828, Abcam) was used to inhibit the HE4 contained in the culture supernatant from HE4-overexpressing HEK293T cells. After 10 minutes, the plates were rinsed twice in PBS and lysis buffer was added, containing 1% SDS and protease inhibitor cocktail or protease and phosphatase inhibitors from Thermo Scientific for Western blotting to evaluate intracellular signaling. After 24 hours, RLT buffer (RNeasy Plus Mini Kit, Qiagen) was added for quantitative reverse transcription–polymerase chain reaction (PCR) or lysis buffer was added for Western blotting or immunofluorescence staining, as described above, to evaluate fibrosis-related genes and proteins.

## Quantitative Real-Time PCR Analysis

Total RNA was prepared by Qiagen RNeasy kit using manufacturer protocols. cDNA was produced using the PrimeScript RT Master mix (Takara), according to the manufacturer's directions. A quantitative reverse transcription–PCR was performed. Primer sequences are listed in Table S1.

## Western Blot Analysis

Western blot analysis was performed as described previously.<sup>16</sup> Antibodies used were as follows: anti-HE, anti–type I collagen, anti- $\alpha$ SMA, anti-GAPDH, ERK, phosphorylated ERK, Protein Kinase B (Akt), phosphorylated Akt, Smad2/3, phosphorylated Smad2, phosphorylated Smad3, c-Jun-NH2-terminal kinase (JNK), phosphorylated JNK, p38, and phosphorylated p38.

## Immunofluorescence Staining for Fibroblast Phenotyping

Immunofluorescence staining was performed as described Data S1. To assess the degree of differentiation, cells were double stained for F-actin using rhodamine-phalloidin (1:1000 dilution, P1951-1MG, Sigma) and for  $\alpha$ SMA using an antibody against  $\alpha$ SMA (1:500 dilution, No. 102M4804V, Sigma), to characterize stress fibers. The coverslips were mounted using Prolong Gold antifade with 4',6-diamidino-2-phenylindole (1:1000, NX034, Dojindo). Degree of differentiation was evaluated by counting the number of cells positive for either F-actin or  $\alpha$ SMA stress fibers in 3 randomly chosen images with a minimum of 80 cells counted per sample. Results from these 3 samples were averaged.

## Statistical Analysis

All data are presented as individual samples with mean values or as mean $\pm$ SD. Unpaired *t* tests or Mann-Whitney *U* tests were used to compare groups. HE4, B-type natriuretic peptide, high-sensitivity cardiac troponin T, and CRP (C-reactive protein) concentrations showed skewed distributions and are therefore expressed as median (interquartile range) and log transformed before Pearson correlation analysis, linear and logistic regression, and Cox regression analysis, when appropriate. Categorical and noncontinuous variables were presented as frequencies or percentages and compared via  $\chi^2$  test. Echocardiographic parameters at baseline and those at follow-up period were compared using a paired *t* test. The Kaplan-Meier method, log-rank test, and the simple and multiple Cox regression analyses were used to assess prognostic association. Unpaired *t* tests were used to compare the collagen area fractions (collagen area/total area) used to estimate cardiac fibrosis between the high and low HE4 groups. Pearson correlation was used to analyze the correlation between the collagen area fraction and serum HE4 levels. The significance level of a statistical hypothesis test was set at  $P < 0.05$ . All data were statistically analyzed using the Statistical Package for the Social Sciences v24 for Windows (SPSS Japan Inc) or GraphPad Prism 8.0. In regard to the basic



**Table 1. Baseline Characteristics of the Study Patients**

Characteristics	All (n=87)	High HE4 (n=43)	Low HE4 (n=44)	P value
Age, y	60±15	64±15	56±13	0.006
Male sex, n (%)	62 (71)	31 (71)	31 (71)	0.866
NYHA functional class, n (%)				
I	21 (24)	7 (16)	14 (32)	
II	44 (51)	19 (44)	25 (57)	
III	16 (18)	12 (28)	4 (9)	
IV	6 (7)	5 (12)	1 (2)	
≥III	22 (25)	17 (40)	5 (11)	0.003
Body mass index, kg/m <sup>2</sup>	23.8±4.2	23.1±4.0	24.5±4.4	0.123
Systolic blood pressure on admission, mm Hg	114±17.2	109±14	118±19	0.012
Hypertension, n (%)	30 (35)	15 (35)	15 (34)	0.938
Diabetes mellitus, n (%)	15 (17)	8 (19)	7 (16)	0.701
Dyslipidemia, n (%)	34 (40)	14 (33)	20 (47)	0.186
Current smoking, n (%)	14 (16)	6 (14)	8 (18)	0.592
Atrial fibrillation, n (%)	22 (25)	14 (33)	8 (18)	0.123
Ventricular tachycardia, n (%)	20 (23)	11 (26)	9 (21)	0.570
Ventricular fibrillation, n (%)	3 (3)	3 (7)	0 (0)	0.075
Prior HF hospitalizations, n (%)	31 (36)	21 (49)	10 (23)	0.011
Laboratory examination parameters				
White blood cell, /μL	6387±1938	6319±1885.7	6455±2007.2	0.746
Hemoglobin, g/dL	14.2±2.16	13.6±2.31	14.8±1.83	0.008
hs-cTnT, ng/mL	0.015 (0.009–0.030)	0.023 (0.015–0.043)	0.011 (0.007–0.016)	0.004
BNP, pg/mL	249.0 (72.7–654.3)	446.0 (194.0–987.1)	134.9 (31.0–480.1)	<0.0001
Albumin, g/dL	3.9±0.5	3.8±0.5	4.1±0.3	<0.0001
Sodium, mEq/L	139±2.6	139±3.1	140±1.7	0.050
Creatinine, mg/dL	0.93±0.27	1.03±0.31	0.84±0.17	0.001
eGFR, mL/min×m <sup>2</sup>	65±15.4	58±15.9	72±11.4	<0.0001
T-bil, mg/dL	1.0±0.59	1.1±0.75	0.93±0.37	0.149
CRP, mg/mL	0.13 (0.05–0.36)	0.18 (0.10–0.63)	0.06 (0.03–0.22)	0.003
HbA1c (NGSP), %	5.8±0.7	5.9±0.8	5.7±0.7	0.331
Medications at baseline, n (%)				
β-Blockers on admission	51 (59)	27 (63)	24 (55)	0.435
β-Blockers on discharge	83 (95)	42 (98)	41 (93)	0.317
ACE-I or ARB on admission	59 (68)	33 (77)	26 (59)	0.078
ACE-I or ARB on discharge	84 (97)	43 (100)	41 (93)	0.081
Aldosterone antagonist on admission	34 (39)	23 (54)	11 (25)	0.006
Aldosterone antagonist on discharge	54 (62)	28 (65)	26 (59)	0.563
Diuretics on admission	44 (51)	25 (58)	19 (43)	0.163
Tolvaptan on admission	3 (4)	2 (6)	1 (3)	0.474
Anticoagulant on admission	23 (26)	15 (35)	8 (18)	0.077
Statin on admission	11 (13)	5 (12)	6 (14)	0.778
Amiodarone on admission	11 (13)	8 (19)	3 (7)	0.098
Pimobendane on admission	4 (5)	3 (7)	1 (2)	0.306
ECG parameters				
Heart rate, bpm	78±18.5	79±20	76±17	0.514
CLBBB, n (%)	13 (15)	9 (21)	4 (9)	0.121

(Continued)

**Table 1. Continued**

Characteristics	All (n=87)	High HE4 (n=43)	Low HE4 (n=44)	P value
QRS duration, ms	114.5±29.3	118.9±33.8	110.3±23.7	0.168
Echocardiogram parameters				
LVEF, %	33±10.7	30±10.7	35±10.1	0.020
LVEDD, mm	60±8.7	61±9.4	59±8.0	0.339
LVESD, mm	51±10.2	53±11.0	50±9.1	0.162
Intraventricular septal thickness, mm	9.3±1.6	9.4±1.7	9.3±1.5	0.859
LV posterior wall thickness, mm	10.0±1.6	10.1±1.8	9.8±1.4	0.420
LAD, mm	42±8.2	43±8.8	40±7.4	0.114
	<b>All (n=78)</b>	<b>High HE4 (n=39)</b>	<b>Low HE4 (n=39)</b>	<b>P value</b>
Right heart catheterization				
Cardiac index, L/min per m <sup>2</sup>	2.2±0.58	2.13±0.51	2.29±0.65	0.236
Pulmonary capillary wedge pressure, mm Hg	15±8.1	16±9.0	14±7.1	0.213
Right atrium pressure, mm Hg	7±3.8	8±4.5	6±3.0	0.148
Mean pulmonary arterial pressure, mm Hg	22±9.9	24±11.2	20±8.2	0.117
	<b>All (n=77)</b>	<b>High HE4 (n=35)</b>	<b>Low HE4 (n=42)</b>	<b>P value</b>
Cardiac magnetic resonance				
LGE, n (%)	39 (51)	18 (51)	21 (50)	1.000

Data are number (percentage) of patients, mean±SD, or median (interquartile range). High HE4 group, above median value of HE4 (median, 59.65 pmol/L); low HE4 group, under median value of HE4. ACE-I indicates angiotensin-converting enzyme inhibitor; ARB, angiotensin receptor blocker; BNP, B-type natriuretic peptide; bpm, beats per minute; CLBBB, complete left bundle-branch block; CRP, C-reactive protein; eGFR, estimated glomerular filtration rate; HbA1c, hemoglobin A1c; HE4, human epididymis protein 4; HF, heart failure; hs-cTnT, high-sensitivity cardiac troponin T; LAD, left atrium diameter; LGE, late gadolinium enhancement; LV, left ventricular; LVEDD, LV end-diastolic diameter; LVEF, LV ejection fraction; LVESD, LV end-systolic diameter; NGSP, National Glycohemoglobin Standardization Program; NYHA, New York Heart Association; and T-bil, total bilirubin.

science experiments, all values were presented as the mean±SD. Differences between groups were analyzed by the Welch *t* test with multiple comparison correction (Bonferroni method).

## RESULTS

### Patient Clinical Characteristics

Baseline characteristics of control and DCM groups are listed in Table S2. Patients in the control group were older than those in the DCM group in our cohort. Fewer patients in the control group had underlying renal or cardiovascular disease, including atrial fibrillation. In the DCM group, the LVEF was significantly lower (33% versus 65%;  $P<0.0001$ ), whereas the LVEDD was significantly higher (60 versus 44 mm;  $P<0.0001$ ). Median serum HE4 levels of the DCM group were significantly higher compared with those of the control group (59.65 versus 44.1 pmol/L;  $P<0.0001$ ) (Figure S2).

Patients with DCM were divided into high and low HE4 groups, using the median values (Table 1). Patients in the high HE4 group were older than those in the low HE4 group (64 versus 56 years;  $P=0.006$ ) and had a higher incidence of prior HF-related

hospitalizations (21 [49%] versus 10 [23%];  $P=0.011$ ). There were no significant differences in sex or the prevalence of coronary risk factors between the 2 groups. Patients in the high HE4 group had higher serum creatinine, CRP, high-sensitivity cardiac troponin T, and plasma B-type natriuretic peptide levels. Patients in the high HE4 group also had lower hemoglobin and serum albumin levels compared with the low HE4 group. Echocardiographic findings, including LVEDD (61 versus 59 mm;  $P=0.339$ ), were not significantly different between the 2 groups at entry point, although LVEF was lower in the high HE4 group (30% versus 35%;  $P=0.020$ ). The prevalence of late gadolinium enhancement in CMR did not differ between the 2 groups. However, Masson trichrome–stained sections from endomyocardial biopsy revealed that the degree of cardiac fibrosis, as estimated by the collagen area fraction, was positively correlated with serum HE4 levels (Figure 1). Most of the study participants were prescribed  $\beta$ -blockers and renin-angiotensin-aldosterone system inhibitors at the time of discharge.

### Association of HE4 With LV Remodeling

Sixty-five patients (29 in the high HE4 group and 36 in the low HE4 group) underwent serial echocardiographic



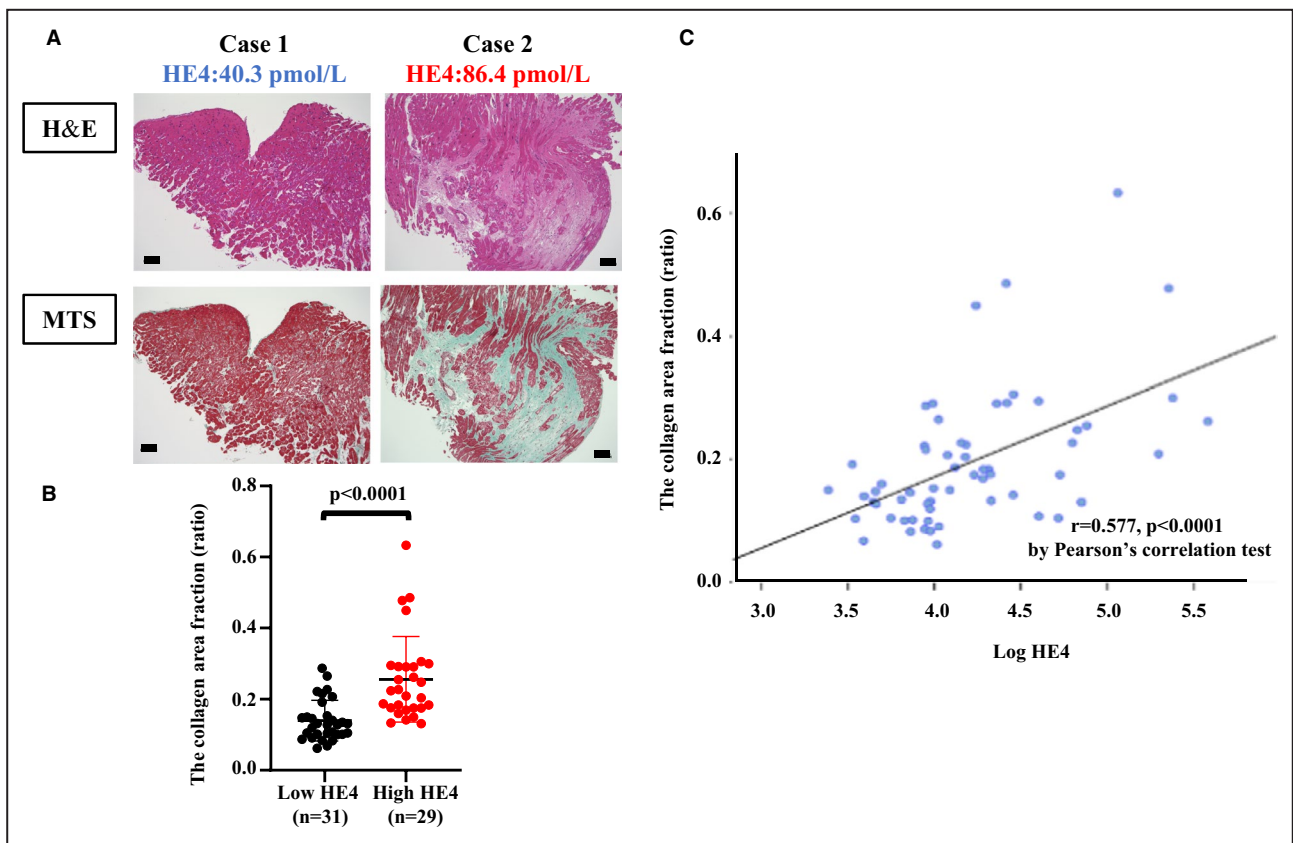


**Figure 1.** Circulating levels of HE4 (human epididymis protein 4) were associated with the degree of cardiac fibrosis in patients with dilated cardiomyopathy.

**A**, Representative microscopic images of cardiac tissue biopsy stained with hematoxylin and eosin (H&E) and Masson trichrome staining (MTS). **B**, The collagen area fraction in the high and low HE4 groups was compared using Mann-Whitney *U* test. **C**, The correlation between ratio of collagen area fraction/serum HE4. Bar=100  $\mu$ m.

assessments during a median follow-up period of 639 days after diagnosis of DCM (Table 2). Follow-up echocardiography showed slight or insignificant improvement in LV remodeling and function compared with baseline data in the high HE4 group. However, in the low HE4 group, LV dimensions were decreased and LVEF was drastically elevated, establishing a possible link between HE4 and ongoing cardiac fibrosis. Multivariate

linear regression analysis showed that HE4 correlated significantly with  $\Delta$ LVEDVi and  $\Delta$ LVESVi, independent of factors that have an association with LV remodeling (Tables S3 and S4). During follow-up, LVRR was observed in 33 of 65 (50.8%) individuals who underwent serial echocardiography. Univariate and multivariate logistic regression analyses revealed that HE4 was an independent predictor of subsequent LVRR (Table S5).

**Table 2.** Echocardiographic Parameters at Baseline and Follow-Up

Parameters	High HE4 (n=29)			Low HE4 (n=36)		
	Baseline	Follow-up	<i>P</i> value	Baseline	Follow-up	<i>P</i> value
LVEDD, mm	59±7.6	58±9.3	0.095	58±7.3	51±6.6	<0.0001
LVESD, mm	51±9.6	48±12.6	0.035	49±8.5	38±8.1	<0.0001
LVEF, %	33±11.1	39±14.0	0.006	35±9.5	49±9.4	<0.0001
LVEDVi, mL/m <sup>2</sup>	97±34.1	90±34.6	0.118	90±28.7	59±14.6	<0.0001
LVESVi, mL/m <sup>2</sup>	68±30.7	59±32.4	0.034	59±22.8	31±10.2	<0.0001
LAD, mm	42±7.8	43±7.9	0.426	40±7.4	38±7.0	0.011

Values are mean±SD. The parameters at baseline and follow-up were compared using a paired *t* test. HE4 indicates human epididymis protein 4; LAD, left atrium diameter; LVEDD, left ventricular end-diastolic diameter; LVEDVi, left ventricular end-diastolic volume index; LVEF, left ventricular ejection fraction; LVESD, left ventricular end-systolic diameter; and LVESVi, left ventricular end-systolic volume index.

## The Prognostic Value of HE4

During the follow-up period, 22 of 87 (25%) patients died or were hospitalized for HF events; 4 of 87 (4.6%) patients died, 4 of 87 (4.6%) patients required LV assist device implantation, and 14 of 87 (16.1%) patients were hospitalized for HF decompensation. The Kaplan-Meier curve demonstrated a significantly higher probability of cardiovascular hospitalization and all-cause mortality in the high HE4 group compared with the low HE4 group (Figure 2A and 2B). As shown in Table 3 and Table S6, Cox regression analysis demonstrated that HE4 was significantly associated with risk reduction of mortality and cardiovascular hospitalization.

## Circulating HE4 Was Derived Mainly From Kidney in the Mouse HF Models

We examined the roles of HE4 in pathophysiology of cardiac fibrosis and first examined the expression profile of HE4 by quantitative reverse transcription-PCR in WT BALB/cA male mice and our 2 mouse models of HFrEF, the genetically induced DCM model and the myocardial infarction-induced model. By echocardiography, mice in both models showed significantly larger LV dimensions and lower LV contraction compared with control mice (Tables S7 and S8). HE4 was scarcely expressed in heart tissues and was highly expressed in kidney tissue of WT mice

in physiological condition (Figure S3A). These data showed similar findings to that of a previous study.<sup>17</sup> Furthermore, the expression of HE4 in kidney tissue was increased in these 2 HFrEF models (Figure S3B and S3C), although those in heart, lung, and liver tissue were not increased. These data suggested that the main source of circulating HE4 in situation of HFrEF is not so much the heart, but instead other organs, such as kidney.

## Distant Organ-Derived HE4 Also Activated Cardiac Fibroblasts and Induced Type I Collagen Deposition

Accordingly, to examine the role of HE4 as a mediator of multiorgan linkage, the culture supernatant of HE4 that overexpressed HEK293T cells (Figure S4A) was transferred to rat neonatal cardiomyocytes and cardiac fibroblasts. Changes in gene and protein expression and intracellular signaling related to pathological hypertrophy, fibrosis, and fibroblast differentiation were examined. Increased HE4 was observed by both quantitative reverse transcription-PCR and Western blotting analyses of culture medium after overexpression of HE4 in HEK293T cells (Figure S4B and S4C). In contrast, mRNAs of major proinflammatory and fibrotic cytokines, such as tumor necrosis factor- $\alpha$ , transforming growth factor- $\beta$ 1, and interleukin-6, were not increased (Figure S4D).

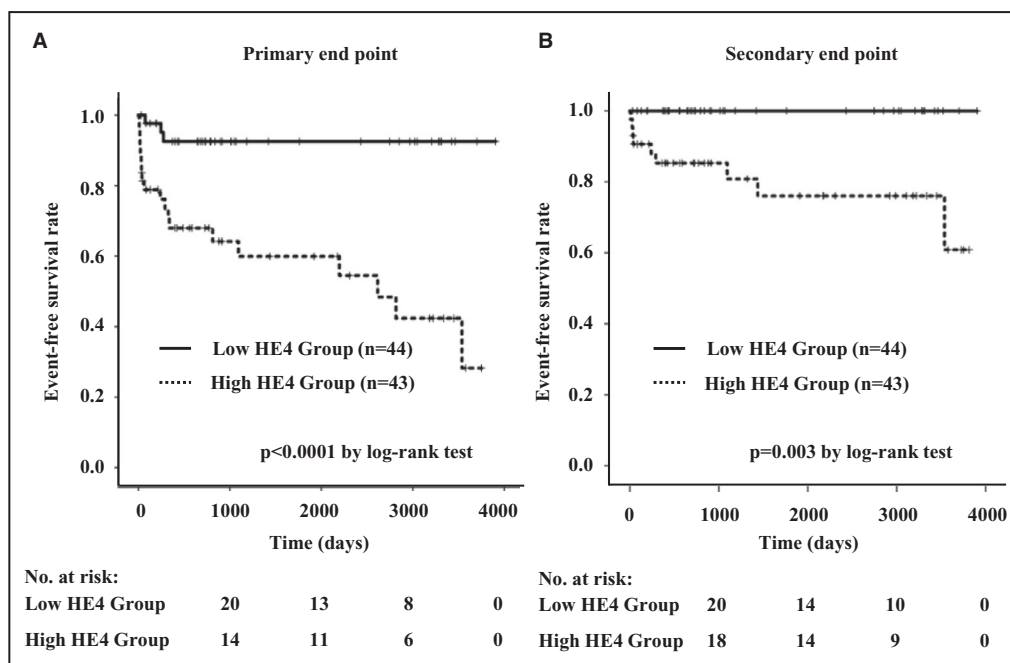


**Figure 2.** Elevated levels of serum HE4 (human epididymis protein 4) were associated with a high risk of future cardiovascular events.

Kaplan-Meier analysis for the probability of primary end point (A) and secondary end point (B) in patients with high and low HE4 levels. Primary end point: composite of all-cause death, left ventricular assist device (LVAD) implantation, and hospitalization for heart failure events. Secondary end point: composite of all-cause death and LVAD implantation.

**Table 3. Univariate Cox Regression Analysis for the Primary End Point**

Variable	Univariate analysis		
	HR	95% CI	P value
Log HE4	5.85	2.77–12.35	<0.0001
Age, y	1.00	0.97–1.03	0.818
NYHA functional class ≥III (yes)	2.90	1.24–6.74	0.014
Systolic blood pressure, mm Hg	0.96	0.93–0.99	0.013
Heart rate, bpm	1.01	0.99–1.04	0.309
Prior HF hospitalizations (yes)	4.39	1.79–10.80	0.001
Atrial fibrillation (yes)	1.34	0.54–3.34	0.526
Log BNP	1.51	1.05–2.15	0.025
Albumin, g/dL	0.44	0.17–1.12	0.084
Hemoglobin, g/dL	0.97	0.81–1.17	0.764
Sodium, mEq/L	0.78	0.69–0.88	<0.0001
Log creatinine	9.05	2.02–40.6	0.004
T-bil, mg/dL	2.43	1.22–4.85	0.012
Log CRP	1.36	1.02–1.83	0.037
QRS duration, ms	1.01	0.99–1.02	0.165
CLBBB (yes)	1.44	0.53–3.93	0.476
LVEF, %	0.94	0.90–0.99	0.015
LVEDD, mm	1.09	1.04–1.15	<0.0001
LVESD, mm	1.09	1.04–1.14	<0.0001
LGE (yes)	2.74	0.97–7.72	0.057

BNP indicates B-type natriuretic peptide; bpm, beats per minute; CLBBB, complete left bundle-branch block; CRP, C-reactive protein; HE4, human epididymis protein 4; HF, heart failure; HR, hazard ratio; LGE, late gadolinium enhancement; LVEDD, left ventricular end-diastolic diameter; LVEF, left ventricular ejection fraction; LVESD, left ventricular end-systolic diameter; NYHA, New York Heart Association; and T-bil, total bilirubin.

Next, addition of the supernatant of HE4-overexpressing HEK293T cells enhanced expression of type I collagen protein in cardiac fibroblast (Figure 3A through 3C). Moreover, mRNA expression of myofibroblast markers, such as  $\alpha$ SMA and SM22 (smooth muscle protein 22), and fibrosis-related genes was also elevated in those cells (Figure 3D). The immunofluorescence revealed that addition of HE4 overexpressed medium-induced  $\alpha$ SMA-positive myofibroblast transdifferentiation (Figure 3E and 3F). Meanwhile, addition of the supernatant that contained HE4 showed no elevations of hypertrophy-related gene expression in cardiomyocytes (Figure S5A and S5B). Prior studies have shown that proinflammatory and fibrotic factors, such as transforming growth factor- $\beta$ 1 and interleukin-6, drive canonical and non-canonical intracellular signaling and induce ongoing fibrosis.<sup>18</sup> We found that ERK was activated by the addition of the supernatant that contained HE4 (Figure 4A and 4B). On the other hand, there were no significant differences in phosphorylation of Smad2 nor in activation of p38 MAP (mitogen-activated protein) kinase, Akt, and JNK (Figure S6A). We then used

U0126, an MEK1/2 inhibitor, to inhibit the activation of ERK. ERK phosphorylation in cardiac fibroblasts was markedly attenuated by treatment with 10  $\mu$ mol/L U0126 (Figure S6B). As shown in Figure 4C and 4D, the increase in protein expression of type I collagen by addition of supernatant that contained HE4 was completely inhibited by U0126 treatment. Furthermore, an anti-HE4 antibody was used to exclude the possibility that factors other than HE4, contained within the supernatant, induced these phenotypes, as previously reported.<sup>19</sup> ERK activation and enhanced fibroblast differentiation by addition of the supernatant were obviously inhibited by anti-HE4 antibody treatment (Figure 4E through 4H). These data suggest that distant organ-derived HE4 facilitated cardiac fibroblast activation through ERK signaling and can lead to ongoing fibrosis in the heart. In other words, HE4 is an independent key driver of fibrosis involving linkage of multiple organs and ongoing fibrosis (Figure 5).

## DISCUSSION

The main findings of the present study were as follows: (1) the high HE4 group showed a lower rate of LVRR; (2) high serum HE4 was associated with future adverse cardiovascular events; (3) upregulated HE4 gene expression in kidney accompanied HFrEF; and (4) HEK293T cell-derived HE4 enhanced the expression of fibrosis-related genes and protein in cardiac fibroblasts, which was accompanied by activation of ERK. Our present findings are thus all compatible with the hypothesis that HE4 is involved in an endocrine manner in cardiac fibrosis and remodeling, and that circulating serum HE4 could be a useful biomarker for the detection of ongoing cardiac fibrosis in patients with DCM.

LVRR has a favorable prognostic value in cardiac diseases.<sup>20</sup> However, methods to predict future LVRR have not been established. In the present study, we found that HE4 was specifically expressed in activated fibroblasts, or “myofibroblasts,” and that serum levels of HE4 had a direct correlation with disease severity and with the degree of cardiac interstitial fibrosis in patients with DCM. More interestingly, the present study also showed that HE4 can serve as a significant predictor of the degree of future LVRR, making it unique compared with conventional markers that reflect past rather than ongoing fibrosis. Ultimately, measurement of circulating HE4 levels could potentially contribute to a novel treatment strategy aimed at LVRR in patients with HF.

To date, there have been 2 studies investigating the prognostic impact of HE4 in patients with HF. These studies showed that HE4 concentration correlated with disease severity and poor prognosis in patients with

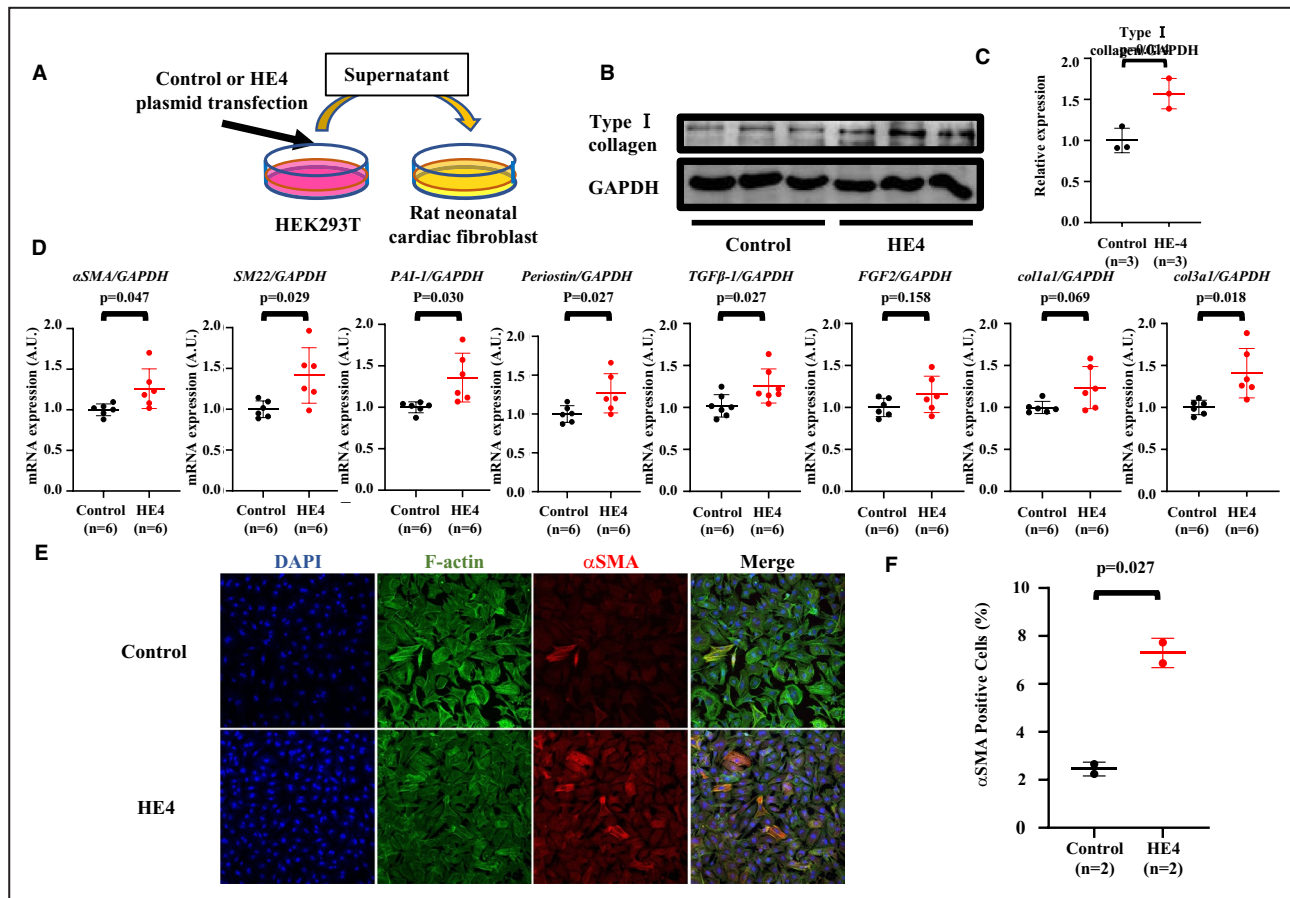


**Figure 3. Cell-secreted HE4 (human epididymis protein 4) induced fibroblast activation and extracellular matrix deposition in cardiac fibroblasts.**

**A**, Experimental scheme for HE4 overexpression and transfer to cardiac fibroblast. **B**, Western blotting (WB) for type I collagen in whole cell lysate of cardiac fibroblast stimulated by culture medium of human embryonic kidney 293T (HEK293T) cells. GAPDH was used as an internal control. **C**, Quantification of WB analysis. **D**, Quantitative reverse transcription–polymerase chain reaction analysis in cardiac fibroblast cultured with supernatant of HEK293T cells. The measurements were standardized to expression of the GAPDH. **E**, Overlay of images of cells stained for 4',6-diamidino-2-phenylindole (DAPI) (blue), F-actin (green), and  $\alpha$ -smooth muscle actin ( $\alpha$ SMA) (red). **F**, Quantification of  $\alpha$ SMA-positive cells as percentage of all cells.  $n=2$  for control,  $n=2$  for HE4. Unpaired  $t$  tests with Welch correction were used to compare groups. Col1a1 indicates collagen 1a1; col3a1, collagen 3a1; FGF2, fibroblast growth factor 2; PAI-1, plasminogen activator inhibitor-1; SM22, smooth muscle protein 22; and TGF- $\beta$ 1, transforming growth factor- $\beta$ 1.

acute and chronic HF, and could improve risk assessment in those patient populations.<sup>21,22</sup> However, they did not evaluate the underlying mechanism of those results. In our present study, the serum HE4 concentration quantified the magnitude of cardiac fibrosis and future LV structural change. In addition, we investigated the role of HE4 in the pathophysiology of HF by in vivo and in vitro experiments. Our in vitro data demonstrated that HE4 activates cardiac fibroblasts and promotes extracellular matrix deposition as an endocrine factor. In addition, our in vivo data suggested HFrEF itself induced HE4 upregulation in kidney regardless of the means of induction of HFrEF. The data from the in vitro and in vivo study may shed light on the novel mechanism of cardiorenal association via circulating HE4.

Matrix metalloproteinases and tissue inhibitor of matrix metalloproteinases are key factors in cardiac

extracellular matrix turnover.<sup>6,23</sup> HE4 has 2 WAP domains consisting of disulfide linkages and can function as an inhibitor of multiple proteinases. Indeed, a previous study showed that HE4 suppressed matrix metalloproteinase expression in fibrotic kidney.<sup>9</sup> Unlike these previous reports, however, we found that HE4 directly induced differentiation from fibroblast to myofibroblast and increased collagen deposition. Furthermore, we examined the underlying mechanism of HE4-induced fibroblast activation and revealed the involvement of ERK signaling, which has been reported to trigger cardiac fibroblast proliferation, leading to cardiac fibrosis.<sup>18</sup> Furthermore, the profibrotic phenotype induced by the supernatants from HE4 overexpressing HEK293T cells was inhibited by anti-HE4 antibody, suggesting that HE4 per se acts as a profibrotic factor in these multiorgan linkages. Taken together, our in



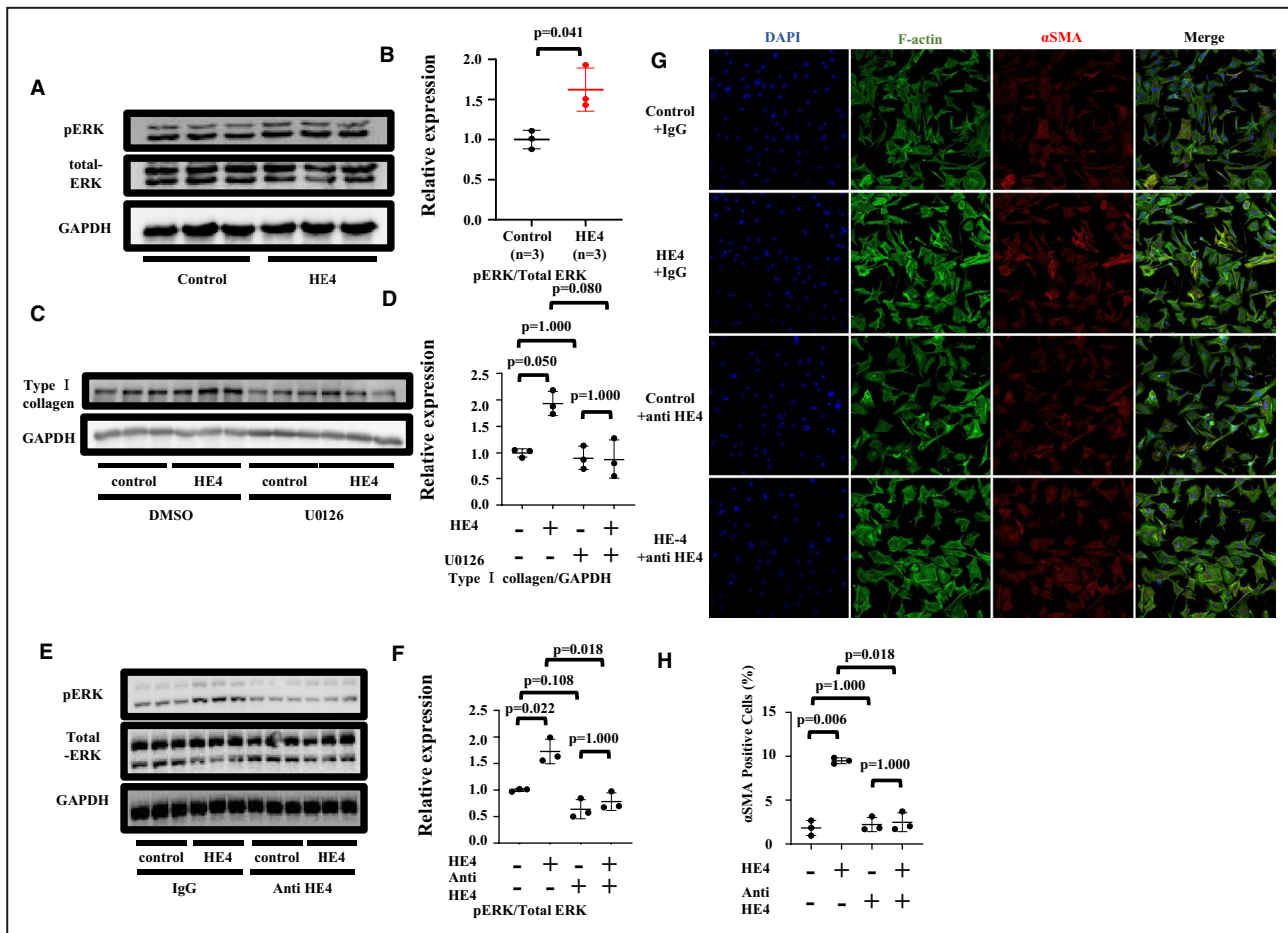


**Figure 4. HE4 (human epididymis protein 4) facilitated cardiac fibroblast activation through extracellular signal-regulated kinase (ERK) signaling.**

**A**, Western blotting (WB) for ERK in cardiac fibroblasts treated with human embryonic kidney 293T (HEK293T) culture medium. **B**, Quantification of phosphorylated ERK (pERK)/total ERK WB analysis. **C**, WB for type I collagen in whole cell lysate of cardiac fibroblast stimulated by culture medium of HEK293T cells, and U0126 or dimethyl sulfoxide (DMSO). GAPDH was used as an internal control. **D**, Quantification of WB analysis. **E**, WB for ERK in whole cell lysate of cardiac fibroblast stimulated by culture medium of HEK293T cells, and anti-HE4 antibody or IgG. GAPDH was used as an internal control. **F**, Quantification of WB analysis. **G**, Overlay of images of fibroblast cultured with supernatant of HEK293T cells, and anti-HE4 antibody or IgG stained for 4',6-diamidino-2-phenylindole (DAPI) (blue), F-actin (green), and α-smooth muscle actin (αSMA) (red). **H**, Quantification of αSMA-positive cells as percentage of all cells. n=3 for control, n=3 for HE4. Unpaired *t* tests with Welch correction and multiple comparison correction (Bonferroni method) were used to compare each group.

vitro data suggest that HE4 exerts a profibrotic effect through ERK-dependent signaling. Although previous studies have shown the profibrotic effect of HE4 in kidney tissue, to the best of our knowledge, this is the first report revealing pathophysiological role of HE4 in cardiac fibrosis.

In the present cohort, although the HF medications were optimized in both the high and low HE4 groups, only the low HE4 group showed significant future LVRR and low adverse events. These clinical findings, in conjunction with our experimental findings described above, suggest that inhibition of HE4 can lead to favorable outcomes. In fact, previous studies have reported that inhibition of HE4 led to the amelioration of the kidney fibrosis.<sup>9</sup> The utility of HE4

in the clinical setting as a potential cardiac fibrosis-reducing therapy may lead to novel treatment strategies for patients with DCM.

We acknowledge several limitations of the current study. First, this was a retrospective single-center study with a small cohort size and small number of cardiovascular events. Although we performed multivariate analysis to the extent possible, as shown in Table S6, confounding factors have not been completely excluded. Further multicenter studies of larger populations are needed to confirm the present results. Second, given the retrospective nature of the study, gene analysis, myocardial biopsies, follow-up echocardiography, and CMR were not performed uniformly in all patients. So, we should take care in interpreting the results of

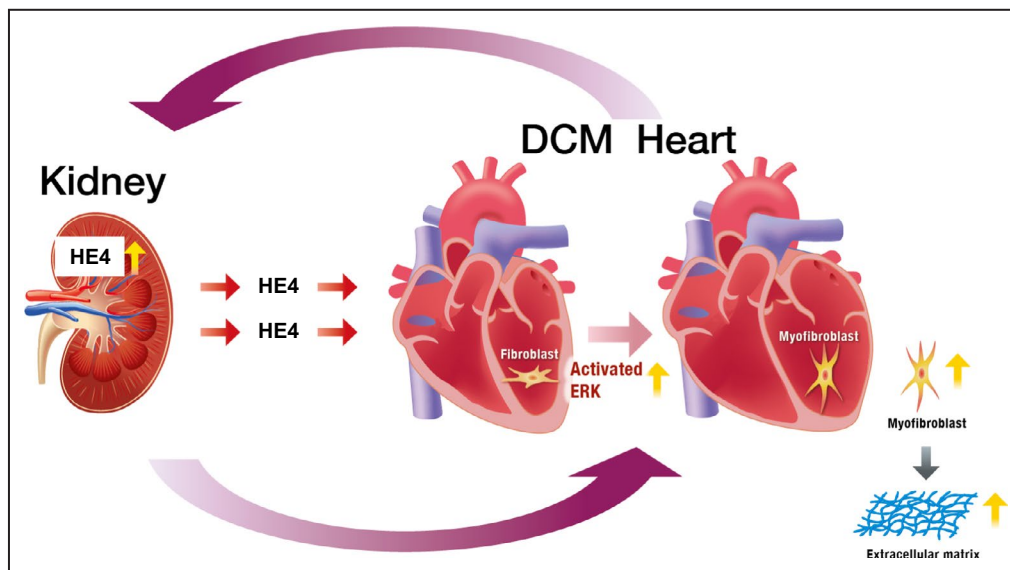


**Figure 5. Vicious cycle of cardiorenal linkage via high HE4 (human epididymis protein 4).** In patients with dilated cardiomyopathy (DCM), HE4 expression is elevated in kidney, and HE4 was secreted into the serum. The circulating HE4 introduced fibroblast activation accompanied by phosphorylation of extracellular signal-regulated kinase (ERK). These were associated with cardiac remodeling and future adverse cardiovascular events.

the details of clinical data. Third, we failed to assess the pathophysiological role of HE4 in cardiac fibrosis in vivo examinations. Further studies are needed to confirm the involvement of HE4 to cardiac fibrosis using HE4-null mouse. Finally, our in vitro analysis was limited as we did not examine the signal cascades related to the profibrotic property of HE4. To address these limitations and to validate our above findings, a large-scale DCM patient analysis and more detailed basic science evaluations are warranted to further validate the present findings.

## CONCLUSIONS

The present study demonstrated that in patients with DCM, circulating levels of HE4 were associated with cardiac remodeling and future adverse cardiovascular events and that HE4 contributed to the cardiac fibrosis or remodeling. These data suggest that HE4 has great potential as both a biomarker of ongoing cardiac fibrosis and a novel therapeutic target for patients with DCM.

## ARTICLE INFORMATION

Received March 7, 2021; accepted June 14, 2021.

### Affiliations

Department of Cardiovascular Medicine, Faculty of Life Sciences (M.Y., S.H., S.A., Y.I., T.Y., N.N., T. Ishida, S.Y., Y.K., Y.A., T.N., S.T., E.Y., K.S., K.K., K.M., K.T.), International Research Center for Medical Sciences (Y.A.), Department of Pathology and Experimental Medicine, Faculty of Life Sciences (T. Ito) and Center for Metabolic Regulation of Healthy Aging (K.T.), Kumamoto University, Kumamoto, Japan; Department of Cardiovascular Medicine,

Osaka City University Graduate School of Medicine, Osaka, Japan (Y.I.); and Department of Health Sciences Fukuoka, International University of Health and Welfare, Fukuoka, Japan (S.M.).

### Acknowledgments

We thank Saeko Tokunaga and Megumi Nagahiro for their excellent technical assistance.

### Sources of Funding

This study was supported, in part, by a Grant-in-Aid for Young Scientists B (16K19412) to Dr Hanatani, and a Grant-in-Aid for Young Scientists (18K15852) to Dr Kimura from the Ministry of Education, Science, and Culture.

### Disclosures

None.

### Supplementary Material

Data S1  
Tables S1–S8  
Figures S1–S6  
Reference 24

## REFERENCES

- Virani SS, Alonso A, Benjamin EJ, Bittencourt MS, Callaway CW, Carson AP, Chamberlain AM, Chang AR, Cheng S, Delling FN, et al. Heart disease and stroke statistics-2020 update: a report from the American Heart Association. *Circulation*. 2020;141:e139–e596. DOI: 10.1161/CIR.0000000000000757.
- Volpe GJ, Moreira HT, Trad HS, Wu KC, Braggion-Santos MF, Santos MK, Maciel BC, Pazin-Filho A, Marin-Neto JA, Lima JAC, et al. Left ventricular scar and prognosis in chronic chagas cardiomyopathy. *J Am Coll Cardiol*. 2018;72:2567–2576. DOI: 10.1016/j.jacc.2018.09.035.
- Merlo M, Pyxaras SA, Pinamonti B, Barbati G, Di Lenarda A, Sinagra G. Prevalence and prognostic significance of left ventricular reverse remodeling in dilated cardiomyopathy receiving tailored medical treatment. *J Am Coll Cardiol*. 2011;57:1468–1476. DOI: 10.1016/j.jacc.2010.11.030.
- Dal Ferro M, Stolfo D, Altinier A, Gigli M, Perrieri M, Ramani F, Barbati G, Pivetta A, Brun F, Monserrat L, et al. Association between mutation



- status and left ventricular reverse remodelling in dilated cardiomyopathy. *Heart*. 2017;103:1704–1710. DOI: 10.1136/heartjnl-2016-311017.
5. Burke MA, Chang S, Wakimoto H, Gorham JM, Conner DA, Christodoulou DC, Parfenov MG, DePalma SR, Eminaga S, Konno T, et al. Molecular profiling of dilated cardiomyopathy that progresses to heart failure. *JCI Insight*. 2016;1:e86898. DOI: 10.1172/jci.insight.86898.
  6. Nagaraju CK, Robinson EL, Abdesslem M, Trenson S, Dries E, Gilbert G, Janssens S, Van Cleemput J, Rega F, Meyns B, et al. Myofibroblast phenotype and reversibility of fibrosis in patients with end-stage heart failure. *J Am Coll Cardiol*. 2019;73:2267–2282. DOI: 10.1016/j.jacc.2019.02.049.
  7. Meyer K, Hodwin B, Ramanujam D, Engelhardt S, Sarikas A. Essential role for premature senescence of myofibroblasts in myocardial fibrosis. *J Am Coll Cardiol*. 2016;67:2018–2028. DOI: 10.1016/j.jacc.2016.02.047.
  8. Vita T, Grani C, Abbasi SA, Neilan TG, Rowin E, Kaneko K, Coelho-Filho O, Watanabe E, Mongeoni FP, Farhad H, et al. Comparing CMR mapping methods and myocardial patterns toward heart failure outcomes in nonischemic dilated cardiomyopathy. *JACC Cardiovasc Imaging*. 2019;12:1659–1669. DOI: 10.1016/j.jcmg.2018.08.021.
  9. LeBleu VS, Teng Y, O'Connell JT, Charytan D, Muller GA, Muller CA, Sugimoto H, Kalluri R. Identification of human epididymis protein-4 as a fibroblast-derived mediator of fibrosis. *Nat Med*. 2013;19:227–231. DOI: 10.1038/nm.2989.
  10. Yancy CW, Jessup M, Bozkurt B, Butler J, Casey DE Jr, Drazner MH, Fonarow GC, Geraci SA, Horwich T, Januzzi JL, et al. 2013 ACCF/AHA guideline for the management of heart failure: a report of the American College of Cardiology Foundation/American Heart Association Task Force on Practice Guidelines. *J Am Coll Cardiol*. 2013;62:e147–e239. DOI: 10.1016/j.jacc.2013.05.019.
  11. Lang RM, Bierig M, Devereux RB, Flachskampf FA, Foster E, Pellikka PA, Picard MH, Roman MJ, Seward J, Shanewise JS, et al. Recommendations for chamber quantification: a report from the American Society of Echocardiography's Guidelines and Standards Committee and the Chamber Quantification Writing Group, developed in conjunction with the European Association of Echocardiography, a branch of the European Society of Cardiology. *J Am Soc Echocardiogr*. 2005;18:1440–1463. DOI: 10.1016/j.echo.2005.10.005.
  12. Verdonschot JAJ, Hazebroek MR, Wang P, Sanders-van Wijk S, Merken JJ, Adriaansen YA, van den Wijngaard A, Krapels IPC, Brunner-La Rocca H-P, Brunner HG, et al. Clinical phenotype and genotype associations with improvement in left ventricular function in dilated cardiomyopathy. *Circ Heart Fail*. 2018;11:e005220. DOI: 10.1161/CIRCHEARTFAILURE.118.005220.
  13. Araki S, Izumiya Y, Rokutanda T, Ianni A, Hanatani S, Kimura Y, Onoue Y, Senokuchi T, Yoshizawa T, Yasuda O, et al. Sirt7 contributes to myocardial tissue repair by maintaining transforming growth factor-beta signaling pathway. *Circulation*. 2015;132:1081–1093. DOI: 10.1161/CIRCULATIONAHA.114.014821.
  14. Yamamura S, Izumiya Y, Araki S, Nakamura T, Kimura Y, Hanatani S, Yamada T, Ishida T, Yamamoto M, Onoue Y, et al. Cardiomyocyte Sirt (Sirtuin) 7 ameliorates stress-induced cardiac hypertrophy by interacting with and deacetylating GATA4. *Hypertension*. 2020;75:98–108. DOI: 10.1161/HYPERTENSIONAHA.119.13357.
  15. Nonaka M, Morimoto S, Murayama T, Kurebayashi N, Li L, Wang YY, Arioka M, Yoshihara T, Takahashi-Yanaga F, Sasaguri T. Stage-dependent benefits and risks of pimobendan in mice with genetic dilated cardiomyopathy and progressive heart failure. *Br J Pharmacol*. 2015;172:2369–2382. DOI: 10.1111/bph.13062.
  16. Shiojima I, Yefremashvili M, Luo Z, Kureishi Y, Takahashi A, Tao J, Rosenzweig A, Kahn CR, Abel ED, Walsh K. Akt signaling mediates postnatal heart growth in response to insulin and nutritional status. *J Biol Chem*. 2002;277:37670–37677. DOI: 10.1074/jbc.M204572200.
  17. National Center for Biotechnology Information. WFDC2 WAP four-disulfide core domain 2 [Homo sapiens (human)]. Gene ID: 10406, updated on June 11, 2021. www.ncbi.nlm.nih.gov/gene/10406. Accessed June 17, 2021.
  18. Schafer S, Viswanathan S, Widjaja AA, Lim W-W, Moreno-Moral A, DeLaughter DM, Ng B, Patone G, Chow K, Khin E, et al. IL-11 is a crucial determinant of cardiovascular fibrosis. *Nature*. 2017;552:110–115. DOI: 10.1038/nature24676.
  19. Zhang L, Liu L, Bai M, Liu M, Wei L, Yang Z, Qian Q, Ning X, Sun S. Hypoxia-induced HE4 in tubular epithelial cells promotes extracellular matrix accumulation and renal fibrosis via NF-κB. *FASEB J*. 2020;34:2554–2567. DOI: 10.1096/fj.201901950R.
  20. Ito E, Miyagawa S, Fukushima S, Yoshikawa Y, Saito S, Saito T, Harada A, Takeda M, Kashiwayama N, Nakamura Y, et al. Histone modification is correlated with reverse left ventricular remodeling in nonischemic dilated cardiomyopathy. *Ann Thorac Surg*. 2017;104:1531–1539. DOI: 10.1016/j.athoracsur.2017.04.046.
  21. de Boer RA, Cao Q, Postmus D, Damman K, Voors AA, Jaarsma T, van Veldhuisen DJ, Arnold WD, Hillege HL, Sillje HH. The WAP four-disulfide core domain protein HE4: a novel biomarker for heart failure. *JACC Heart Fail*. 2013;1:164–169. DOI: 10.1016/j.jchf.2012.11.005.
  22. Plek A, Meijers WC, Schroten NF, Gansevoort RT, de Boer RA, Sillje HH. HE4 serum levels are associated with heart failure severity in patients with chronic heart failure. *J Card Fail*. 2017;23:12–19. DOI: 10.1016/j.cardfail.2016.05.002.
  23. Khalil H, Kanisicak O, Vagnozzi RJ, Johansen AK, Maliken BD, Prasad V, Boyer JG, Brody MJ, Schips T, Kilian KK, et al. Cell-specific ablation of Hsp47 defines the collagen-producing cells in the injured heart. *JCI Insight*. 2019;4:e128722. DOI: 10.1172/jci.insight.128722.
  24. Nakayama M, Yamamuro M, Takashio S, Uemura T, Nakayama N, Hirakawa K, Oda S, Utsunomiya D, Kaikita K, Hokimoto S, et al. Late gadolinium enhancement on cardiac magnetic resonance imaging is associated with coronary endothelial dysfunction in patients with dilated cardiomyopathy. *Heart Vessels*. 2018;33:393–402. DOI: 10.1007/s00380-017-1069-1.

# **SUPPLEMENTAL MATERIAL**

## Data S1.

### Supplemental Materials and Methods

<i>Procedure and Follow up of clinical study</i>	Blood samples were collected in the stable phase during the first admission, and the serum human epididymis protein 4 (HE4) levels were measured using the CLIA method (Abbott). The coefficient of variation of HE4 among samples was less than 10%. The study primary endpoint was a composite of all-cause death, left ventricular assist device (LVAD) implantation, and hospitalization for heart failure (HF) events. Furthermore, composite of all-cause death and LVAD implantation were defined as secondary endpoint. Death, LVAD implantation and heart failure events were identified by searching the medical records and confirmed by direct contact with the patients, relatives, and caring physicians.
<i>Echocardiography of clinical study</i>	Left ventricular end-diastolic diameter (LVEDD), left ventricular end-systolic diameter (LVESD), thickness of the interventricular septum, posterior ventricular wall and left atrial diameter were obtained from M-mode or two-dimensional images of parasternal long axis views. Left ventricular end-diastolic volume (LVEDV) and left ventricular end-systolic were (LVESV) were measured in apical 4-and 2-chamber windows by the Simpson method. Left ventricular (LV) ejection fraction (LVEF) was calculated by the modified Simpson method (Vivid 7®; GE-Vingmed Ultrasound).
<i>Statistical analysis of Echo data</i>	Univariable linear regression and logistic regression analysis for $\Delta$ LVEDVi (follow-up LVEDVi – baseline LVEDVi), $\Delta$ LVESVi (follow-up LVESVi – baseline LVESVi), and left ventricular reverse remodeling (LVRR) was performed using HE4 and other variables involved in LV remodeling. <sup>12</sup> Multivariable analysis was performed using the variables achieving significance at $p < 0.05$ on univariable analysis or clinically important variables to determine the factors associated with $\Delta$ LVEDVi, $\Delta$ LVESVi, and LVRR. LVRR was defined as the combined presence of: (1) an increase in LVEF of at least 10 points or a follow-up LVEF $\geq 50\%$ ; and (2) a decrease in LVEDDi of at least 10% or an LVEDDi $\leq 33$ mm/m. <sup>3</sup>
<i>CMR image acquisition and Image analysis</i>	66 patients (76%) underwent cardiac magnetic resonance (CMR) and were checked for the presence of late gadolinium enhancement (LGE). All images were acquired using a 3.0 T scanner (Achieva 3.0 T X-series TX; Philips Medical Systems). We used electrocardiogram-gated cine imaging techniques with a segmented steady-state free precession sequence in the short and three

	<p>long cardiac axes with LGE imaging as described previously.<sup>24</sup> Approximately 10 min after injection of 0.1 mmol/kg of a gadolinium-based contrast agent (Magnevist; Bayer Healthcare), we acquired two-dimensional inversion-recovery sequences, including the LV from base to apex. CMR images were independently analyzed by a cardiologist and a radiologist. Patients were then classified into LGE-positive or -negative groups.<sup>24</sup></p>
<p><i>Mouse models and Procedures</i></p>	<p>Wild-type (WT) male mice on a BALB/cA background were used in this study. All procedures were performed in accordance with the Kumamoto University animal care guidelines, which conform to the Guide for the Care and Use of Laboratory Animals published by the US National Institutes of Health (publication No. 85-23, revised 1996). The study was approved by the Animal Research Ethics Committee of Kumamoto University (#A2019-122). WT male mice with BALB/cA background were purchased from Kyudo company (Saga, Japan). The mice were housed in a temperature- and humidity-controlled (24°C) room on a 12 h light/dark cycle. The 8-week-old mice were anesthetized with isofluran. The mouse myocardial infarction (MI) model was generated as previously described.<sup>13, 14</sup> Briefly, the trachea was cannulated with a polyethylene tube connected to a respirator (tidal volume, 0.6 mL; frequency, 110 breaths per minute). A left thoracotomy was performed between the fourth and fifth ribs. The pericardial tissue was removed, and the left anterior descending artery was visualized under a microscope and permanently ligated with 7-0 silk suture. Sham-operated mice underwent surgery but not left anterior descending artery ligation. At 4 weeks after MI surgery, mouse body weight, echocardiographic data, and urine output were analyzed prior to sacrifice. The mouse DCM model was generated using knock-in mice on the genetic background of BALB/cJ, in which three base-pairs coding for K210 in cTnT were deleted from the endogenous Tnnt2 gene as previously described.<sup>15</sup> 5 Homozygous mutant mice and WT mice were obtained by crossing heterozygous mutant mice, and were used as DCM and control models, respectively. MI surgery model and six-week old DCM model mouse were anesthetized with overdose isoflurane, and hearts, kidney, lung and liver were rapidly excised, and freeze clamped for subsequent analyses. <i>In vivo</i> analysis and post-euthanasia myocardial histological and molecular analyses were performed by investigators who were blinded to the experimental groups.</p>

<p><i>Echocardiography, in vivo</i></p>	<p>At 1 day before harvest, echocardiography was performed using the Xario system (Toshiba, Tokyo, Japan) with a 12-MHz linear array transducer. Heart rates and respiratory rates were continuously monitored. LV wall thickness and LV systolic and diastolic dimensions were measured in M-mode. LV percent fractional shortening were calculated. These analyses were performed by investigators who were blinded to the mice models.</p>
<p><i>Cell culture, harvest and incubation of neonatal rat cardiomyocytes and fibroblasts</i></p>	<p>Primary neonatal rat cardiomyocytes and fibroblasts were isolated from 2-day-old Wistar rats (Japan SLC, Inc). The hearts were harvested and minced and allowed to digest in 1 mg/ml Type II collagenase (Sigma Chemical Co.). After digestion, cardiomyocytes and fibroblasts were separated by Percoll density gradient centrifugation and incubated under 5% CO<sub>2</sub> and 37°C in 1 g/L glucose Dulbecco's Modified Eagle's Medium (DMEM) containing 10% fetal bovine serum (FBS), ampicillin (10 U/μl), streptomycin (10 μg/μl), and amphotericin B (25 μg/ml).</p>
<p><i>Quantitative real time PCR analysis</i></p>	<p>RNA was extracted using a RNeasy Mini Kit (QIAGEN). cDNA synthesis was performed using PrimeScript RT Master mix (TAKARA) according to the manufacturer's directions. A quantitative reverse-transcription polymerase chain reaction (qRT-PCR) was carried out for Co11a1, Co13a1, alpha smooth muscle actin (αSMA), plasminogen activator inhibitor-1 (PAI-1), fibroblast growth factor 2 (FGF2), smooth muscle protein 22 (SM22), periostin, fibronectin, transforming growth factor-β1 (TGF-β1), tumor necrosis factor-α (TNF-α), and interleukin-6 (IL-6). The reactions were carried out in technical duplicates. Primers were utilized with SYBR Green PCR Master Mix (BIO-RAD) in CFX384 Real-Time System (BIO-RAD). The data processing is based on a standard curve-based method for relative qRT-PCR. Measurements were standardized to expression of glyceraldehyde-3-phosphate dehydrogenase (GAPDH) or 18S. For <i>in vivo</i> studies, qRT-PCR was carried out for HE4 and GAPDH. <b>Table S1</b> lists the primer sequences used in this study.</p>
<p><i>Western blot analysis</i></p>	<p>Cells were scraped and lysed with 1% SDS lysis buffer containing protease inhibitor cocktail (Thermo). The samples were centrifuged at 20400 g for 15 min. The supernatant was collected, and protein concentrations were determined using a Pierce BCA Protein assay Kit (Code: 23225, Thermo). After proteins were transferred to a PVDF Blotting membrane (GE Healthcare Life Sciences), the membrane was blocked with 100 mM Tris-HCl, pH 7.5, 0.9% NaCl, and 0.1% Tween 20 (TBST) containing 5% nonfat dry milk for 1 hour and then</p>

	<p>incubated with primary antibodies at 4°C overnight. The primary antibodies were as follows: anti-HE4 (ab200828, Abcam), anti-type I collagen (#84336S, 1, CST), anti-<math>\alpha</math>SMA (ab5694, Abcam), anti-GAPDH (#2118, CST), ERK (#9102, CST), p-ERK (#4377, CST), Akt (#9272, CST), p-Akt (#9271, CST), Smad2/3 (#8685, CST), p-Smad2 (#18338, CST), p-Smad3 (#9520, CST), JNK (#9252, CST), p-JNK (#9251, CST), p38 (#9211, CST), p-p38 (#4511, CST). Membranes were then incubated with HRP-secondary antibodies for 1 hour at room temperature. Immunoreactive proteins were detected using ECL Prime (GE Healthcare UK Ltd.) with LAS-4000 Imaging system (FUJIFILM).</p>
<p><i>Immunofluorescence staining for fibroblast phenotyping in vitro</i></p>	<p>After 24 hours in culture, cells were fixed with 4% paraformaldehyde diluted in PBS for 20 minutes at room temperature. Further, cells were permeabilized with 0.1% Triton X-100. To assess the degree of differentiation, cells were double stained for F-actin using rhodamine-phalloidin (1:1000 dilution, P1951-.1MG, Sigma) and for <math>\alpha</math>-smooth muscle actin, using an antibody against <math>\alpha</math>SMA (1:500 dilution, #102M4804V, Sigma), to characterize stress fibers. The coverslips were mounted using Prolong Gold anti-fade with DAPI (1:1000, NX034, Dojindo). Fluorescence imaging was done using a confocal microscope TCS SP8 LS with 20X/0.4 objective. Degree of differentiation was evaluated by counting the number of cells positive for either F-actin or <math>\alpha</math>SMA stress fibers in three randomly chosen images with a minimum of 80 cells counted per sample. Results from these 3 samples were averaged.</p>



**Table S1. Primer sequences used for quantitative real-time PCR.**

	<b>Forward Primer</b>	<b>Reverse Primer</b>
HE4 (human)	CCCAATGATAAGGAGGGT	ATTCATCTGGCCAGGAC
HE4 (mouse)	AACCAATTACGGACTGTGTGTT	TCGCTCGGTCCATTAGGCT
$\alpha$ SMA (rat)	GGGATCCTGACCCTGAAG	AGTGGTGCCAGATCTTTT
PAI-1 (rat)	ACATCCTGGAAGTGCCT	TGGTCATGTTGCTCTTCC
FGF2 (rat)	CGCCTGGAGTCCAATAAC	ACAGTATGGCCTTCTGTC
SM22 (rat)	GGAACAGGTGGCTCAATTCT	CCCAAAGCCATTACAGTCCT
collagen1a1 (rat)	GATGGACTCAACGGTCTC	GGCAGGAAGCTGAAGTCA
collagen3a1 (rat)	ATGCATGTTTCTCCGGTTT	CTCGGAATTGCAGAGACC
TGF- $\beta$ 1 (rat)	CGGACTACTACGCCAAAG	TCCCCGAATGTCTGACGT
TGF- $\beta$ 1 (human)	GCGTGCTAATGGTGGAAACC	GCTTCTCGGAGCTCTGATGT
Periostin (rat)	CAAACCACTTTCACGGACCT	TTGTTACAGGCGCTAACAG
Fibronectin (rat)	CAGCCCCTGATTGGAGTC	TGGGTGACACCTGAGTGAAC
TNF- $\alpha$ (human)	GGACCTCTCTAATCAGCCC	TGAAGAGGACCTGGGAGTAGA
IL-6 (human)	TACATCCTCGACGGCATCTC	TGGCTTGTTCCTCACTACTCT
GAPDH (rat)	TCAAGAAGGTGGTGAAGCAG	AGGTGGAAGAATGGGAGTTG
18S (human)	CGGCTACCACATCCAAGGAA	GCTGGAATTACCGCGGCT
ANP (rat)	AGGCCATATTGGAGCAAATC	CATCTTCTCCTCCAGGTGGT
$\beta$ -MHC (rat)	CTGGCACCGTGGACTACAAT	GCCCTTGTCTACAGGTGCAT

PCR, polymerase chain reaction; HE4, human epididymis protein 4;  $\alpha$ SMA, alpha smooth muscle actin; PAI-1, plasminogen activator inhibitor-1; FGF2, Fibroblast growth factor 2; SM22, smooth muscle protein 22; TGF- $\beta$ 1, Transforming Growth Factor- $\beta$ 1; TNF- $\alpha$ , tumor necrosis factor- $\alpha$ ; IL-6, Interleukin-6; GAPDH, Glyceraldehyde-3-phosphate dehydrogenase; ANP, atrial natriuretic peptides;  $\beta$ -MHC,  $\beta$ -myosin heavy chain

**Table S2. Baseline characteristics of the control and DCM groups.**

	Control (n = 59)	DCM (n = 87)	<i>p</i> value
HE4, pmol/L	44.1 [35.6-52.9]	59.65 [49.0-86.2]	<0.0001
Age, y	69 ± 3	60 ± 15	<0.0001
Male sex, n (%)	30 (51)	62 (71)	0.012
Body Mass Index, kg/m <sup>2</sup>	23.8 ± 3.9	23.8 ± 4.2	0.902
Systolic blood pressure on admission, mmHg	123 ± 17	114 ± 17.4	0.002
Hypertension, n (%)	36 (61)	30 (35)	0.002
Diabetes mellitus, n (%)	17 (29)	15 (17)	0.105
Dyslipidemia, n (%)	43 (73)	34 (40)	<0.0001
Current smoker, n (%)	14 (24)	14 (16)	0.250
Atrial fibrillation, n (%)	3 (5)	22 (25)	0.001
Non-Sustained ventricular tachycardia, n (%)	1 (2)	20 (23)	<0.0001
Ventricular fibrillation, n (%)	0 (0)	3 (3)	0.150
Prior HF hospitalizations, n (%)	0 (0)	31 (36)	<0.0001
Laboratory examination parameters			
White blood cell, /μL	6066 ± 1798.6	6387 ± 1938	0.313
Hemoglobin, g/dL	13.9 ± 1.64	14.2 ± 2.16	0.493
hs-cTnT, ng/mL	0.007 [0.003-0.010]	0.015 [0.009-0.029]	0.013
BNP, pg/mL	16.6 [9.9-29.8]	249.0 [72.7-654.3]	<0.0001
Albumin, g/dL	4.2 ± 0.33	3.9 ± 0.5	<0.0001
Serum sodium, mEq/L	140 ± 1.8	139 ± 2.6	0.011
Creatinine, mg/dL	0.71 ± 0.16	0.93 ± 0.27	<0.0001
eGFR, mL/min*m <sup>2</sup>	76 ± 11.8	65 ± 15.4	<0.0001
T-bil, mg/dL	0.8 ± 0.29	1.0 ± 0.59	0.009

CRP, mg/ml	0.04 [0.02-0.08]	0.13 [0.05-0.36]	0.021
HbA1c (NGSP)	6.0 ± 1.00	5.8 ± 0.7	0.305
Electrocardiogram parameters			
Heart rate, bpm	68 ± 12.1	78 ± 18.5	0.001
CLBBB, n (%)	0 (0)	13 (15)	0.002
QRS duration, msec	99 ± 11.6	114.5 ± 29.3	<0.0001
Echocardiogram parameters			
LVEF, %	65 ± 4.6	33 ± 10.7	<0.0001
LVEDD, mm	44 ± 5.0	60 ± 8.7	<0.0001
LVESD, mm	27 ± 4.2	51 ± 10.2	<0.0001
Intraventricular septal thickness, mm	9.7 ± 1.5	9.3 ± 1.6	0.151
LV posterior wall thickness, mm	9.7 ± 1.6	10.0 ± 1.6	0.348
LVEDVi, ml/L/min/m <sup>2</sup>	38 ± 15.0	97 ± 35.2	<0.0001
LVESVi, ml/L/min/m <sup>2</sup>	13 ± 5.9	67 ± 31.6	<0.0001
LAD, mm	34 ± 5.1	42 ± 8.2	<0.0001

Data are number of patients (%), mean ± standard deviation (SD), and median (interquartile range).

DCM, dilated cardiomyopathy; HE4, human epididymis protein 4; HF, heart failure; hs-cTnT, high-sensitivity cardiac troponin T; BNP, B-type natriuretic peptide; eGFR, estimated glomerular filtration rate; T-bil, total bilirubin; CRP, c-reactive protein; CLBBB, complete left bundle branch block; LVEF, left ventricular ejection fraction; LVEDD, left ventricular end-diastolic diameter; LVESD, left ventricular end-systolic diameter; LV, left ventricular; LVEDVi, left ventricular end-diastolic volume index; LVESVi, left ventricular end-systolic volume index; LAD, left atrium diameter

**Table S3. Univariate and multivariate linear regression analyses of  $\Delta$ LVEDVi.**

	Univariate Analysis		Multivariate Analysis	
	$\beta$ -coefficient	<i>p</i> Value	$\beta$ -coefficient	<i>p</i> Value
Log (HE4), per 1 pmol/L increment	0.344	0.006	0.518	0.001
Age, per 1-year increment	0.086	0.499	-0.094	0.484
NYHA class $\geq$ III	-0.089	0.484		
Systolic blood pressure on admission, 1 mmHg increment	0.007	0.954		
Hypertension	-0.091	0.473		
Diabetes mellites	-0.029	0.818		
$\beta$ -blocker on discharge	-0.209	0.098	-0.166	0.188
ACE-I or ARB on discharge	-0.092	0.469		
Log (BNP), per 1 pg/mL increment	-0.133	0.294	-0.194	0.168
Log (Creatinine), per 1 mg/dL increment	-0.033	0.794	-0.192	0.146
eGFR, per 1 mL/(min $\cdot$ m <sup>2</sup> ) increment	-0.053	0.677		
Log (CRP), per 1 mg/m increment	0.107	0.407		
QRS duration, per 1 mm increment	-0.057	0.657		
CLBBB	0.104	0.412		
LVEF, per 1 % increment	0.299	0.017		
LVEDD, mm	-0.381	0.002	-0.359	0.009
LVESD, mm	-0.366	0.003		
LGE	0.039	0.778	0.091	0.777

LVEDVi, left ventricular end-diastolic volume index; HE4, human epididymis protein 4; NYHA, New York Heart Association; ACE-I, angiotensin-converting enzyme inhibitor; ARB, angiotensin receptor blocker; BNP, B-type natriuretic peptide; eGFR, estimated glomerular filtration rate; CRP, c-reactive protein; CLBBB, complete left bundle branch block; LVEF, left ventricular ejection fraction; LVEDD, left ventricular end-diastolic diameter; LVESD, left ventricular end-systolic diameter; LGE, late gadolinium enhancement

**Table S4. Univariate and multivariate linear regression analyses of  $\Delta$ LVESVi.**

	Univariate Analysis		Multivariate Analysis	
	$\beta$ -coefficient	<i>p</i> value	$\beta$ -coefficient	<i>p</i> value
Log (HE4), per 1 pmol/L increment	0.344	0.006	0.508	0.001
Age, per 1-year increment	0.086	0.499	-0.072	0.592
NYHA class $\geq$ III	-0.089	0.484		
Systolic blood pressure on admission, 1 mmHg increment	0.007	0.954		
Hypertension	-0.091	0.473		
Diabetes mellites	-0.029	0.818		
$\beta$ -blocker on discharge	-0.209	0.098	-0.153	0.227
ACE-I or ARB on discharge	-0.092	0.469		
Log (BNP), per 1 pg/mL increment	-0.133	0.294	-0.195	0.168
Log (Creatinine), per 1 mg/dL increment	-0.033	0.794	-0.175	0.192
eGFR, per 1 mL/(min*m2) increment	-0.053	0.677		
Log (CRP), per 1 mg/m increment	0.107	0.407		
QRS duration, per 1 mm increment	-0.057	0.657		
CLBBB	0.104	0.412		
LVEF, per 1 % increment	0.299	0.017		
LVEDD, mm	-0.381	0.002		
LVESD, mm	-0.366	0.003	-0.364	0.009
LGE	0.039	0.778	0.109	0.356

LVESVi, left ventricular end-systolic volume index; HE4, human epididymis protein 4; NYHA, New York Heart Association; ACE-I, angiotensin-converting enzyme inhibitor; ARB, angiotensin receptor blocker; BNP, B-type natriuretic peptide; eGFR, estimated glomerular filtration rate; CRP, c-reactive protein; CLBBB, complete left bundle branch block; LVEF, left ventricular ejection fraction; LVEDD, left ventricular end-diastolic diameter; LVESD, left ventricular end-systolic diameter; LGE, late gadolinium enhancement

**Table S5. Univariate and multivariate logistic regression analyses of LVRR positive.**

	Univariate Analysis		Multivariate Analysis	
	B	p value	B	p value
Log (HE4), per 1 pmol/L increment	-0.398	0.001	-0.615	<0.0001
Age, per 1 year increment	-0.209	0.094	-0.032	0.830
NYHA class $\geq$ III	-0.123	0.329		
Systolic blood pressure on admission, 1 mmHg increment	0.163	0.195		
Hypertension	0.150	0.235		
Diabetes mellites	0.072	0.569		
$\beta$ -blocker on discharge	0.003	0.983	0.074	0.584
ACE-I or ARB on discharge	-0.070	0.585		
Log (BNP), per 1 pg/mL increment	0.058	0.646	0.419	0.008
Log (Creatinine), per 1 mg/dL increment	-0.109	0.387	0.241	0.096
eGFR, per 1 mL/(min*m2) increment	0.148	0.238		
Log (CRP), per 1 mg/m increment	-0.151	0.239		
QRS duration, per 1 mm increment	-0.060	0.636		
CLBBB	-0.177	0.158		
LVEF, per 1 % increment	-0.050	0.694		
LVEDD, mm	-0.045	0.721	-0.260	0.068
LVESD, mm	-0.087	0.492		
LGE	0.133	0.329	0.026	0.844

LVRR, left ventricular reverse remodeling; HE4, human epididymis protein 4; NYHA, New York Heart Association; ACE-I, angiotensin-converting enzyme inhibitor; ARB, angiotensin receptor blocker; BNP, B-type natriuretic peptide; eGFR, estimated glomerular filtration rate; CRP, c-reactive protein; LVEF, left ventricular ejection fraction; LVEDD, left ventricular end-diastolic diameter; LVESD, left ventricular end-systolic diameter; LGE, late gadolinium enhancement



**Table S6. Results of multivariate Cox regression analysis for the primary endpoint.**

Factor	Multivariate Analysis		
	HR	95% CI	<i>p</i> value
Model 1			
Log HE4	7.91	3.49-17.94	<0.0001
Age (years)	0.97	0.95-1.00	0.074
Model 2			
Log HE4	5.07	2.25-11.43	<0.0001
NYHA class $\geq$ III	2.12	0.58-3.82	0.405
Model 3			
Log HE4	4.92	2.34-10.35	<0.0001
Systolic blood pressure (mmHg)	0.97	0.93-1.00	0.058
Model 4			
Log HE4	5.09	2.31-11.19	<0.0001
Prior HF hospitalizations (yes)	3.23	1.27-8.21	0.014
Model 5			
Log HE4	4.29	1.85-9.94	0.001
Sodium (mEq/L)	0.90	0.78-1.03	0.130
Model 6			
Log HE4	5.09	2.05-12.64	<0.0001
Log Creatinine	1.57	0.28-8.76	0.606

Model 7			
Log HE4	6.49	2.98-14.14	<0.0001
T-bil (mg/dL)	2.32	1.26-4.28	0.007
Model 8			
Log HE4	6.68	2.43-18.37	<0.0001
Log CRP	0.92	0.64-1.31	0.640
Model 9			
Log HE4	5.16	2.26-11.76	<0.0001
Log BNP	1.16	0.77-1.75	0.474
Model 10			
Log HE4	8.81	3.78-20.51	<0.0001
LVEDD (mm)	1.12	1.06-1.18	<0.0001
Model 11			
Log HE4	9.13	3.78-22.08	<0.0001
LGE (yes)	2.55	0.89-7.31	0.082

---

HR, hazard ratio; HE4, human epididymis protein 4; NYHA, New York Heart Association; HF, heart failure; T-bil, total bilirubin; CRP, c-reactive protein; BNP, B-type natriuretic peptide; LVEDD, left ventricular end-diastolic diameter; LGE, late gadolinium enhancement

**Table S7. Parameters at harvest in BALB/cA WT and genetically induced HFrEF model mice (Homo).**

	WT (n = 7)	Homo (n = 7)	<i>p</i> value
Age, week	6	6	1.000
Body weight, g	18.3 ± 1.15	17.1 ± 1.76	0.134
Heart rate, bpm	715 ± 43.6	681 ± 57.8	0.243
Echocardiogram parameters at 1 day before harvest			
LVEDD, mm	2.63 ± 0.39	4.74 ± 1.03	0.001
LVESD, mm	1.47 ± 0.42	3.91 ± 1.13	0.001
Intraventricular septal thickness, mm	0.59 ± 0.09	0.44 ± 0.05	0.005
LV posterior wall thickness, mm	0.63 ± 0.14	0.36 ± 0.05	0.001
%FS, %	44.6 ± 11.1	18.5 ± 8.93	<0.0001
Organ weight at harvest			
Heart/tibial length, mg/mm	7.07 ± 0.62	13.5 ± 3.63	0.003
Lung/tibial length, mg/mm	8.92 ± 0.80	13.9 ± 5.93	0.070
Kidney/tibial length, mg/mm	8.93 ± 0.62	8.36 ± 0.52	0.091

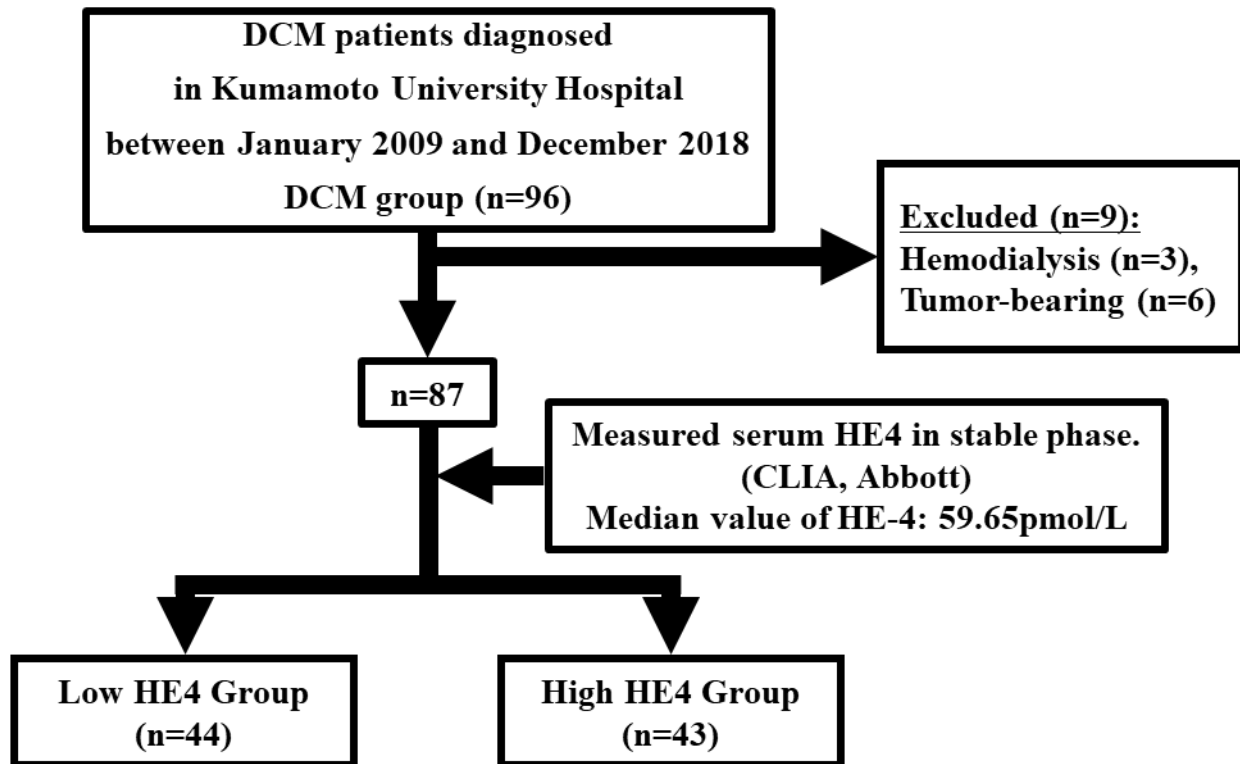
Values are mean ± SD. WT, Wild-type; HFrEF, heart failure with reduced ejection fraction; LVEDD, left ventricular end-diastolic diameter; LVESD, left ventricular end-systolic diameter; LV, left ventricular; %FS, % fractional shortening

**Table S8. Parameters at harvest 4 weeks after MI-induced HFrEF model mice in BALB/cA WT mice.**

	Sham-operated (n = 7)	MI (n = 7)	<i>p</i> value
Age, week	12	12	1.000
Body weight, g	23.8 ± 0.93	23.8 ± 1.41	0.976
Heart rate, bpm	643 ± 59.0	677 ± 41.8	0.241
Echocardiogram parameters at 1 day before harvest			
LVEDD, mm	3.00 ± 0.59	3.71 ± 0.42	0.025
LVESD, mm	1.30 ± 0.51	2.69 ± 0.53	<0.0001
Intraventricular septal thickness, mm	0.63 ± 0.10	0.30 ± 0.10	<0.0001
LV posterior wall thickness, mm	0.64 ± 0.08	0.50 ± 0.12	0.021
%FS, %	58.0 ± 10.2	28.1 ± 7.32	<0.0001
Organ weight at harvest			
Heart/tibial length, mg/mm	8.28 ± 0.76	9.35 ± 1.38	0.103
Lung/tibial length, mg/mm	8.31 ± 0.38	8.58 ± 0.69	0.387
Liver/tibial length, mg/mm	63.5 ± 5.07	66.0 ± 6.72	0.443
Kidney/tibial length, mg/mm	12.3 ± 0.82	12.2 ± 2.03	0.927

Values are mean ± SD. MI, myocardial infarction; HFrEF, heart failure with reduced ejection fraction; WT, Wild-type; LVEDD, left ventricular end-diastolic diameter; LVESD, left ventricular end-systolic diameter; LV, left ventricular; %FS, % fractional shortening

**Figure S1. Flow chart of patient enrollment protocol in the present study.**

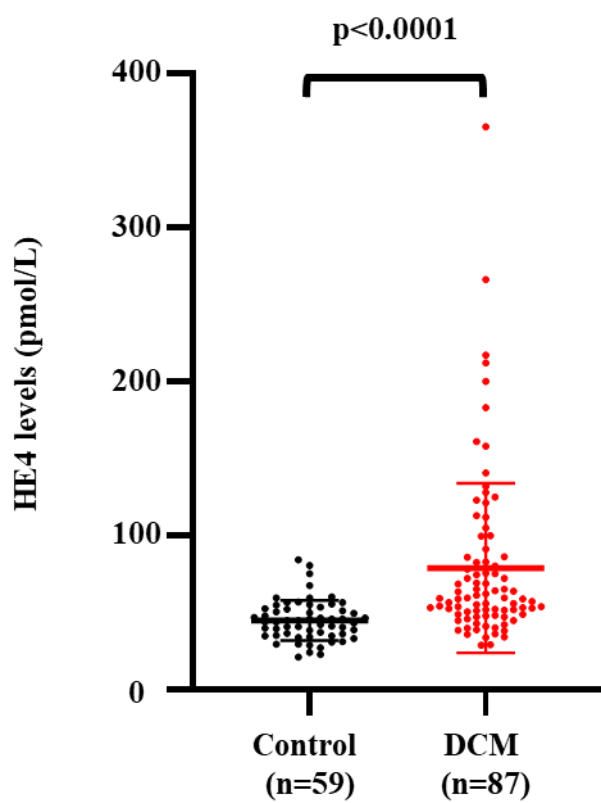


**Followed the data of each patient.**

We excluded 9 patients because they were undergoing hemodialysis or had a tumor. According to the median value of HE4 (59.65 pmol/L), we divided all DCM patients into the high HE4 group (n = 43) and the low HE4 group (n = 44).

HE4: human epididymis protein 4, DCM: dilated cardiomyopathy

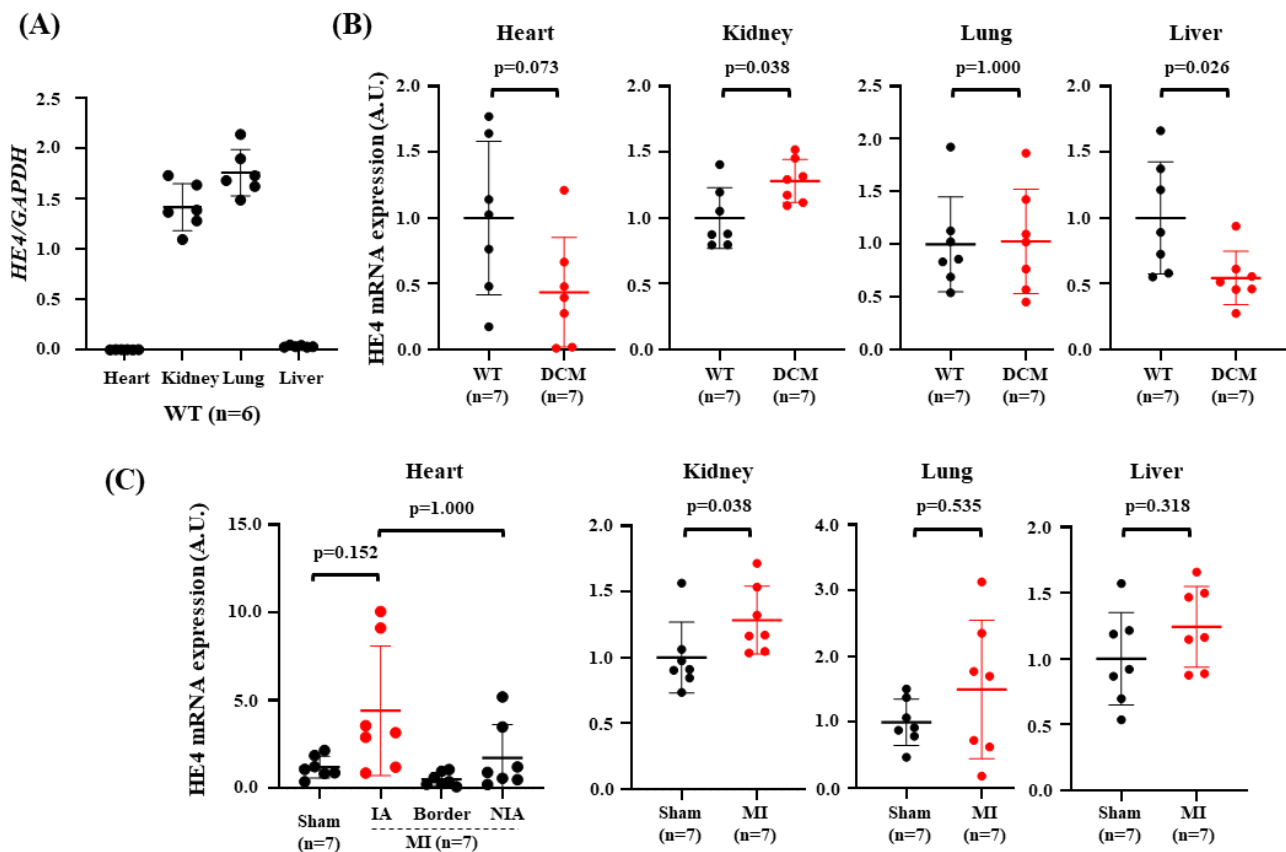
Figure S2. Serum HE4 levels in the control and DCM group.



Unpaired t-tests were used to compare groups.

HE4: human epididymis protein 4, DCM: dilated cardiomyopathy

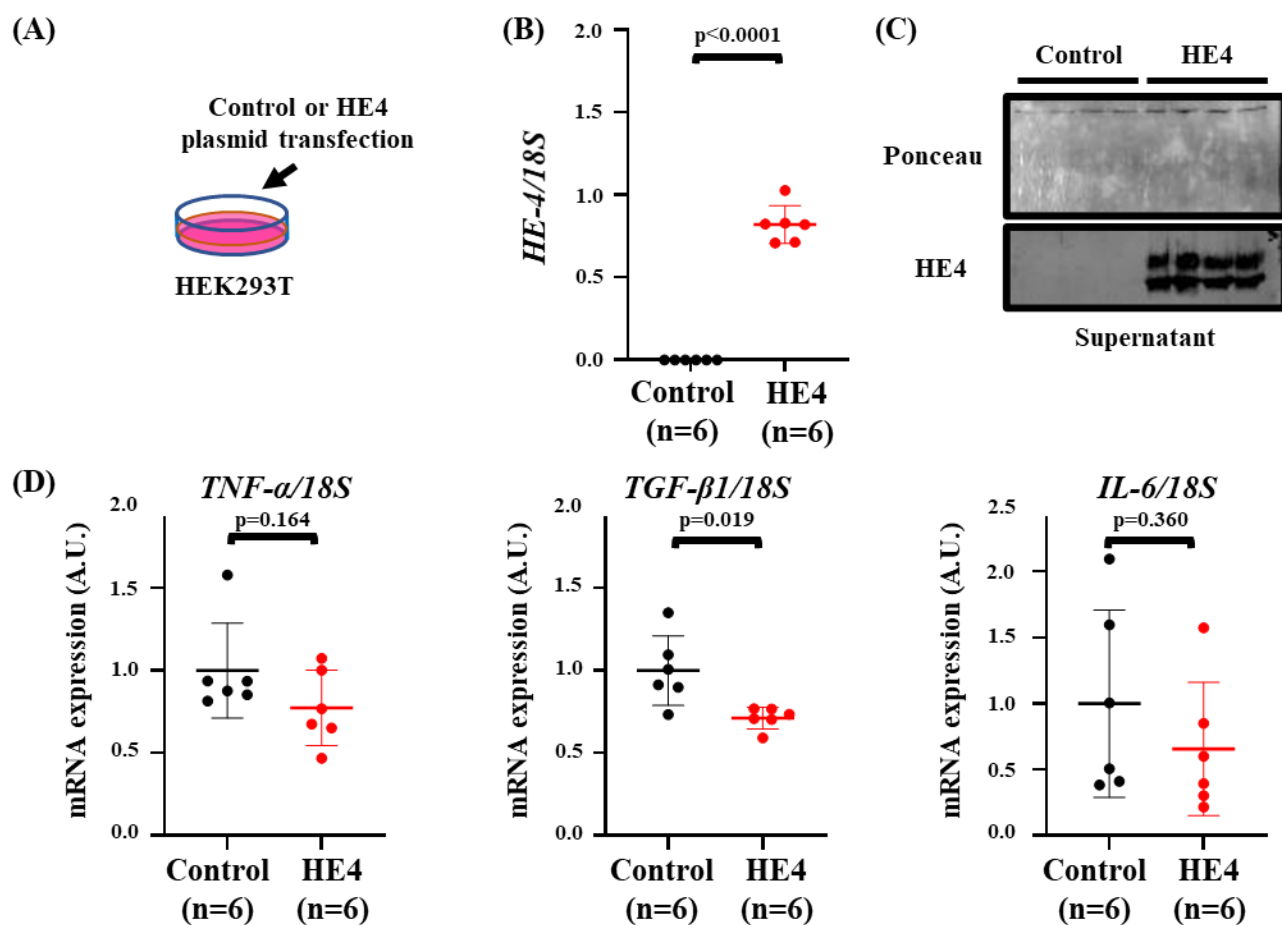
**Figure S3. HE4 is upregulated at kidney tissue in situation of HF/rEF.**



(A) The expression profile of HE4 in the heart, kidneys, lungs, and liver of BALB/cJ WT mice (n = 6). GAPDH was used as an internal control. (B) Quantitative evaluation of HE4 mRNA expression normalized to GAPDH mRNA expression in each tissue from DCM model mice (n = 7) and their WT littermates (n = 7) using the standard curve-method. The ratio of DCM mice to WT mice is shown. (C) Quantitative evaluation of HE4 mRNA expression normalized to GAPDH in heart, kidneys, lungs, and liver from MI model mice (n = 7) and sham operated mice (n = 7) using standard curve-method. The ratio of MI to sham operated mice is shown.

HE4: human epididymis protein 4, WT: wild type, GAPDH: glyceraldehyde-3-phosphate dehydrogenase, MI: myocardial infarction, IA: infarcted area, NIA: non-infarcted area

**Figure S4. Overexpression of HE4 have no impact on the expression of inflammatory-related and fibrosis-related genes in HEK293T cells.**



(A) Experimental scheme for HE4 overexpression. (B) qRT-PCR analysis in HEK293T cells transfected with control or HE4 plasmid. 18S was used as an internal control. (C) WB for HE4 in supernatant of control or HE4 plasmid transfected HEK293T. (D) qRT-PCR analysis in HEK293T cells transfected with control or HE4 plasmid. 18S was used as an internal control.

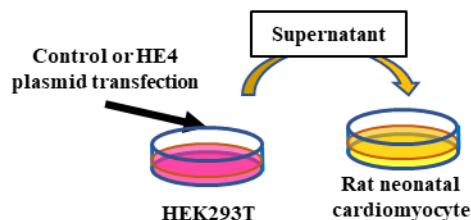
Unpaired t-tests with Welch's correction were used to compare groups.

WB: western blotting, HE4: human epididymis protein 4, HEK293T: human embryonic kidney 293T, qRT-PCR: quantitative reverse-transcription polymerase chain reaction, TNF- $\alpha$ : tumor necrosis factor- $\alpha$ , TGF- $\beta$ 1: transforming growth factor- $\beta$ 1, IL-6: interleukin-6

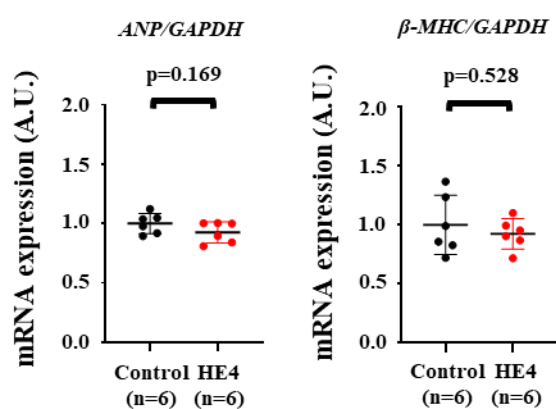


**Figure S5. The addition of the supernatant that contained HE4 show no elevations of hypertrophy-related genes expression in cardiomyocytes.**

(A)



(B)

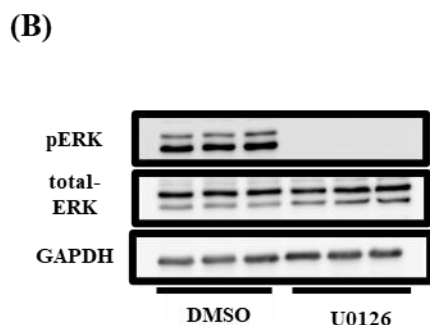
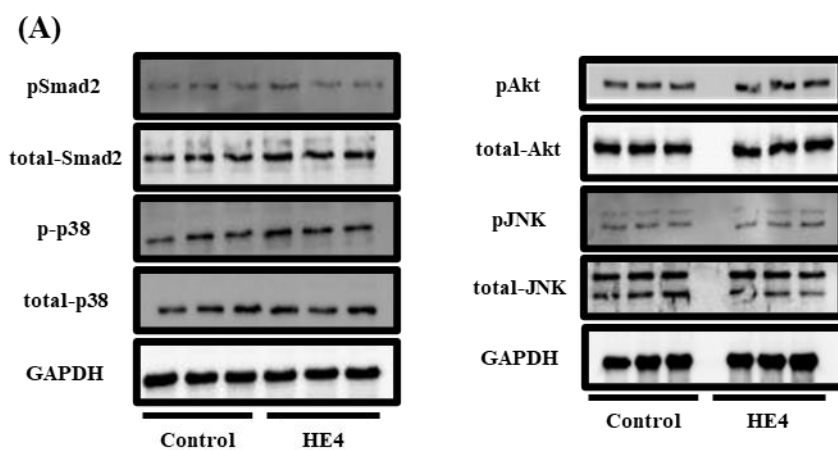


(A) Experimental scheme for HE4 overexpression and transfer to cardiomyocyte. (B) Cardiac hypertrophy-related genes were evaluated by qRT-PCR. The measurements were standardized to expression of the GAPDH.

Unpaired t-tests with Welch's correction were used to compare groups.

HE4: human epididymis protein 4, HEK293T: human embryonic kidney 293T, GAPDH: glyceraldehyde-3-phosphate dehydrogenase, ANP: atrial natriuretic peptides, β-MHC: β-myosin heavy chain, qRT-PCR: quantitative reverse-transcription polymerase chain reaction

**Figure S6. HE4 does not affect the activity of Smad2, p38 MAP kinase, Akt, and JNK**



(A) WB for intracellular signaling other than ERK in cardiac fibroblasts treated with HEK293T culture medium. (B) WB for ERK in cardiac fibroblasts treated with HEK293T culture medium and U0126, MEK 1/2 inhibitor, or DMSO.

WB: western blotting, ERK: extracellular signal-regulated kinase, HE4: human epididymis protein 4, HEK293T: human embryonic kidney 293T, GAPDH: glyceraldehyde-3-phosphate dehydrogenase, DMSO: dimethyl sulfoxide